ORGANOMETALLICS
Article

Organometallics **2009,** *28,* 5445–5458 5445
DOI: 10.1021/om900705v

On the First Insertion of α-Olefins in Hafnium Pyridyl-Amido Polymerization Catalysts

Cristiano Zuccaccia,[†] Vincenzo Busico,[‡] Roberta Cipullo,[‡] Giovanni Talarico,[‡] Robert D. J. Froese,[⊥] Paul C. Vosejpka,[⊥] Phillip D. Hustad,[§] and Alceo Macchioni*[,†]

[†]*Department of Chemistry, University of Perugia, Via Elce di Sotto, 8-06123, Perugia, Italy,* [‡]*Department of Chemistry, University of Napoli, Via Cintia, 80126, Napoli, Italy,* [§]*The Dow Chemical Company, 2301 North Brazosport Boulevard, B-3827, Freeport, Texas 7754, and* [⊥]*The Dow Chemical Company, 1776 Building, Midland, Michigan 48674*

Received August 10, 2009

Reactions of [{N^-,N,$C_{naphthyl}{}^-$}HfMe][$MeB(C_6F_5)_3$] (**2**) precatalyst with a series of α-olefins have been investigated in order to intercept the active polymerization species generated by an *in situ* modification of the precursor by insertion of a single monomer unit into the Hf−C_{Aryl} bond. In all cases the first migratory insertion of monomer occurs into the Hf−C_{Aryl} bond rather than the Hf−C_{Alkyl} bond. A low-temperature polymerization with 170 equiv of 1-hexene activated with tris(pentafluorophenyl)borane (FAB) allows for the complete NMR characterization of a Hf−$C_{Alkylaryl}$ methyl cation. This structure agrees with DFT studies of the kinetically favored diastereomer, although a number of other structures are more stable thermodynamically. Attempts to trap an inserted catalyst through the stoichiometric addition of 2-vinylpyridine or 3-ethoxy-1-propylene led to complicated reactions, but in both cases, experimental and computational data suggest that both processes initiate through insertion of the substrate into the Hf−C_{Aryl} bond. In addition, an activated Hf-dibutyl complex is studied in an attempt to minimize differences in the rates of initiation and propagation, as a butyl group is a reasonable mimic for a propagating polymer chain. Tritylborate activation of this complex cleanly generates 1 equiv of 1-butene in close proximity to the Hf-butyl cation via *β*-hydride abstraction. This reaction results in formation of isotactic poly(1-butene) with a fairly high molecular weight rather than butene oligomers. The observed molecular weight is consistent with a small fraction of active species, and quenching studies show a similar fraction of butene-modified ligand. These results are consistent with slow insertion into the Hf−C_{Aryl} bond followed by fast polymerization kinetics, with the latter rate constant being 3 orders of magnitude faster than the former.

Introduction

Pyridyl-amide complexes have recently demonstrated great promise in the field of olefin polymerization catalysis. Upon activation, these {N^-,N,$C_{Aryl}{}^-$}$HfMe_2$ C_1-symmetric arylcyclometalated hafnium-pyridyl-amido precatalysts[1] lead to extremely efficient catalysts for olefin polymerization. Discovered and optimized through high-throughput parallel screening techniques,[2−4] these species have been successfully applied in high-temperature solution processes for the production of highly isotactic, high molecular weight polypropylene.[5] More recently, these species

*Corresponding author. E-mail: alceo@unipg.it.

(1) {N^-,N,C^-} indicates a tridentate ligand with an anionic Hf-amide (N^-), neutral Hf−pyridyl bond (N), and Hf−$C_{Aryl/Alkyl}$ bonds (C^-).

(2) (a) Boussie, T. R.; Diamond, G. M.; Goh, C.; Hall, K. A.; LaPointe, A. M.; Leclerc, M. K.; Lund, C.; Murphy, V. (Symyx Technologies, Inc.) U.S. Pat. Appl. Publ. No. US 2006/0135722 A1. (b) Boussie, T. R.; Diamond, G. M.; Goh, C.; Hall, K. A.; LaPointe, A. M.; Leclerc, M. K.; Lund, C.; Murphy, V. (Symyx Technologies, Inc.) U.S. Pat. 7,018,949, 2006. (c) Boussie, T. R.; Diamond, G. M.; Goh, C.; LaPointe, A. M.; Leclerc, M. K.; Lund, C.; Murphy, V. (Symyx Technologies, Inc.) U.S. Pat. 6,750,345, **2004**. (d) Boussie, T. R.; Diamond, G. M.; Goh, C.; Hall, K. A.; LaPointe, A. M.; Leclerc, M. K.; Lund, C.; Murphy, V. (Symyx Technologies, Inc.) U.S. Pat. 6,713,577, **2004**. (e) Boussie, T. R.; Diamond, G. M.; Goh, C.; Hall, K. A.; LaPointe, A. M.; Leclerc, M. K.; Lund, C.; Murphy, V. (Symyx Technologies, Inc.) U.S. Pat. 6,706,829, **2004**. (f) Boussie, T. R.; Diamond, G. M.; Goh, C.; Hall, K. A.; LaPointe, A. M.; Leclerc, M. K.; Lund, C.; Murphy, V. (Symyx Technologies, Inc.) PCT Int. Appl. Publ. No. WO 2002/046249. (g) Boussie, T. R.; Diamond, G. M.; Goh, C.; Hall, K. A.; LaPointe, A. M.; Leclerc, M. K.; Lund, C.; Murphy, V. (Symyx Technologies, Inc.) PCT Pat. Appl. Publ. No. WO 2002/038628.

(3) Boussie, T. R.; Diamond, G. M.; Goh, C.; Hall, K. A.; LaPointe, A. M.; Leclerc, M. K.; Lund, C.; Murphy, V.; Shoemaker, J. A.W.; Tracht, U.; Turner, H.; Zhang, J.; Uno, T.; Rosen, R. K.; Stevens, J. C. *J. Am. Chem. Soc.* **2003**, *125*, 4306.

(4) Boussie, T. R.; Diamond, G. M.; Goh, C.; Hall, K. A.; LaPointe, A. M.; Leclerc, M. K.; Murphy, V.; Shoemaker, J. A. W.; Turner, H.; Rosen, R. K.; Stevens, J. C.; Alfano, F.; Busico, V.; Cipullo, R.; Talarico, G. *Angew. Chem., Int. Ed.* **2006**, *45*, 3278.

(5) (a) Arriola, D. J.; Bokota, M.; Timmers, F. J. (Dow Chemical Company) PCT Int. Appl. Publ. No. WO 2004/026925 A1. (b) Frazier, K. A.; Boone, H.; Vosejpka, P. C.; Stevens, J. C. (Dow Chemical Company) U.S. Pat. Appl. Publ. No. US 2004/0220050 A1. (c) Tau, L.-M.; Cheung, Y. W.; Diehl, C. F.; Hazlitt, L. G. (Dow Chemical Company) U.S. Pat. Appl. Publ. No. US 2004/0087751 A1. (d) Tau, L.-M.; Cheung, Y. W.; Diehl, C. F.; Hazlitt, L. G. (Dow Chemical Company) U.S. Pat. Appl. Publ. No. US 2004/0242784 A1. (e) Coalter, J. N., III; Van Egmond, J. W.; Fouts, L. J., Jr.; Painter, R. B.; Vosejpka, P. C. (Dow Chemical Company) PCT Int. Appl. Publ. No. WO 2003/040195 A1. (f) Stevens, J. C.; Vanderlende, D. D. (Dow Chemical Company) PCT Int. Appl. Publ. No. WO 2003/040201 A1.

Published on Web 09/01/2009

Scheme 1. Activation with Brønsted Acids

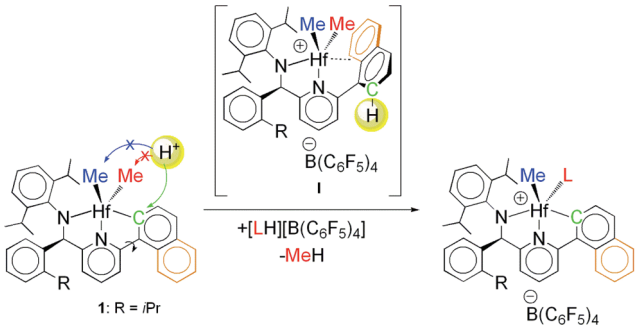

have also found use in the production of a new class of olefin block copolymers through chain shuttling polymerization.[6]

One distinguishing structural feature of these species over most of the other precatalysts for olefin polymerization[7,8] is the presence of both Hf−C_{Alkyl} and Hf−C_{Aryl} bonds. On one hand, the Hf−C_{Aryl} bond plays a key role in determining the outstanding performance of these species,[3] but it also adds several layers of complexity on both the activation and polymerization mechanisms. Particularly, it offers alternatives for both protic attack, in the case of activation with Brønsted acids, and olefin insertion. An in-depth analysis of the molecular weight distributions of polymers generated with the above-mentioned catalysts[9] indicates that polymerizations are carried out by several active sites. It was proposed that these multiple catalytic sites may be derived from this peculiar structural feature.

With the aim of intercepting and identifying the catalytically active sites, we initiated a systematic study of the activation of {N^-,N,C_{Aryl}^-}$HfMe_2$ precatalysts and their subsequent reactions with olefins. The results of the activation studies were reported in a recent article.[10] The activation of these precatalysts with Lewis acids proceeds by methyl abstraction,[10] in line with other metallocene and post-metallocene systems.[11] On the contrary, Brønsted acids, such as $[HNR_3][B(C_6F_5)_4]$, selectively protonate the metalated aryl arm of the tridentate ligand, forming dimethyl intermediate **I** stabilized by an Hf-η^2-naphthyl interaction (Scheme 1).[10] This dimethyl species slowly undergoes naphthyl remetalation assisted by a nucleophile L (Scheme 1).[10]

Activation and 1-alkene polymerization studies using different precatalyst/cocatalyst combinations demonstrate that intermediate **I** is likely more distant from the catalytically active species than the remetalated ion pair.[10] These data suggest that the monomethyl ion pairs bearing the Hf−C_{Aryl} bond are starting points for entering the catalytic cycle. Although these activation studies disclose several important aspects of the peculiar chemistry of {N^-,N,C_{Aryl}^-}$HfMe_2$ compounds, they do not afford any rationalization of their multisite behavior in catalysis. One proposal for the generation of multiple sites again turns to the potential reactivity of the Hf−C_{Aryl} bond. Analogous to protonation during activation with Brønsted acids, the incoming olefin can choose to react with either the Hf−C_{Alkyl} or Hf−C_{Aryl} bonds (Scheme 2).

The former case represents the "classical" migratory insertion reaction, leading to formation of species **AI**, which can continue to insert olefins (Scheme 2, pathway A). On the contrary, a first insertion into the Hf−C_{Aryl} bond (Scheme 2, pathway B) causes a modification of the {N^-,N,C_{Aryl}^-} ligand through formation of **BI**, which can then successively undergo "classical" multiple migratory insertion reactions into the Hf−C_{Alkyl} bond. This possibility was first proposed by Froese et al. to account for multisite behavior in ethylene/octene copolymerizations.[9] Through theoretical calculations, they showed that (i) insertion into the Hf−C_{Aryl} bond has a lower barrier than the corresponding insertion into the Hf−C_{Alkyl} bond and (ii) the monoinserted species **BI** displays several characteristics consistent with polymerization data, including a low barrier to site epimerization.[9] This olefin insertion could result in many different **BI** diastereomers depending on the orientation of the naphthyl moiety and stereochemistry of the insertion in the case of α-olefins. Consequently, **BI** is a good candidate to be one of the active species, but the experimental data do not preclude **2** from also being another.

In addition to computations, some experimental evidence has been found to support pathway B. First, a small fraction of 4-methyl-1-pentene-appended ligand, arising from olefin insertion into the Hf−C_{Aryl} bond, has been isolated and characterized from a 4-methyl-1-pentene polymerization in the presence of **2**.[9] Second, when $^{13}CH_2{=}^{13}CH_2$ was polymerized, the ^{13}C NMR spectra showed resonances at 69 and 35 ppm that are consistent with ethylene insertion into the Hf−C_{Aryl} bond.[9] Related C_s-symmetric achiral precursors produce poly(α-olefins) with prevalently isotactic microstructures and complex multimodal molecular weight distributions.[12−14] Coates and co-workers have also recently synthesized a cationic species having a single chiral sp^3-hybridized carbon bridging the naphthyl moiety and hafnium that produces isotactic polypropylene in a living fashion.[15]

Although these observations are sufficient to establish the viability of pathway B, they do not necessarily demonstrate that the first olefin insertion preferentially occurs into the Hf−C_{Aryl} bond nor that the resulting isomeric ion pairs (**BI**-type) are the main active species. In this article, we describe our experimental attempts to intercept and characterize monoinserted species and possibly evaluate the relative activity of species **2**, **AI**, and **BI**. Careful studies of the

(6) Arriola, D. J.; Carnahan, E. M.; Hustad, P. D.; Kuhlman, R. L.; Wenzel, T. T. *Science* **2006**, *312*, 714.
(7) For a case in which olefin inserts in a Ti−C_{Aryl} bond see: Gielens, E. E. C. G.; Dijkstra, T. W.; Berno, P.; Meetsma, A.; Hessen, B.; Teuben, J. H. *J. Organomet. Chem.* **1999**, *591*, 88.
(8) For another precatalyst for olefin polymerization having both M−C_{Alkyl} and M−C_{Aryl} bonds (M = Ti, Zr, and Hf) see: Tam, K.-H.; Lo, J. C. Y.; Guo, Z.; Chan, M. C. W. *J. Organomet. Chem.* **2007**, *692*, 4750.
(9) Froese, R. D. J.; Hustad, P. D.; Kuhlman, R. L.; Wenzel, T. T. *J. Am. Chem. Soc.* **2007**, *129*, 7831.
(10) Zuccaccia, C.; Macchioni, A.; Busico, V.; Cipullo, R.; Talarico, G.; Alfano, F.; Boone, H. W.; Frazier, K. H.; Hustad, P. D.; Stevens, J. C.; Vosejpka, P. C.; Abboud, K. A. *J. Am. Chem. Soc.* **2008**, *130*, 10354.
(11) Chen, E. Y.-X.; Marks, T. *J. Chem. Rev.* **2000**, *100*, 1391.
(12) Domski, G. J.; Lobkovsky, E. B.; Coates, G. W. *Macromolecules* **2007**, *40*, 3510.
(13) Niu, A.; Stellbrink, J.; Allgaier, J.; Richter, D.; Hartmann, R.; Domski, G. J.; Coates, G. W.; Fetters, L. J. *Macromolecules* **2009**, *42*, 1083.
(14) Busico, V.; Cipullo, R.; Pellecchia, R.; Rongo, L.; Talarico, G.; Macchioni, A.; Zuccaccia, C.; Froese, R. D. J.; Hustad, P. D. *Macromolecules* **2009**, *42*, 4369.
(15) Domski, G. J.; Edson, J. B.; Keresztes, I.; Lobkovsky, E. B.; Coates, G. W. *Chem. Commun.* **2008**, 6137.

Scheme 2. First Migratory Insertion of Olefin in the Hf−C_{Alkyl} (pathway A) or Hf−C_{Aryl} (pathway B) Bonds (P = polymeryl chain)

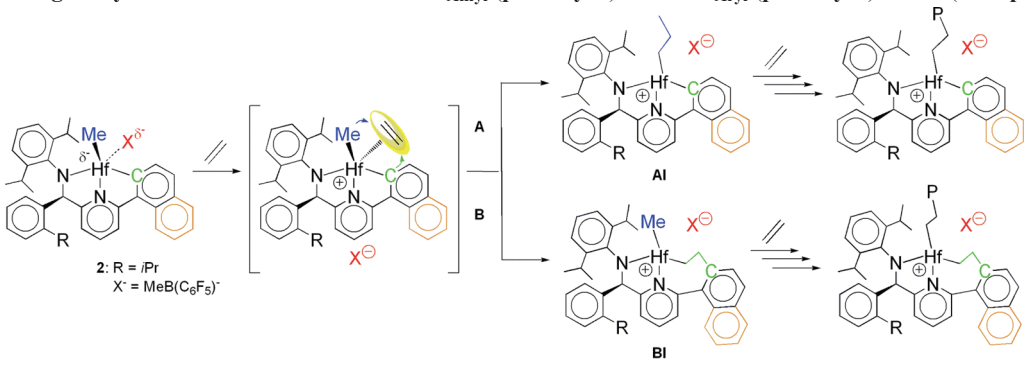

activation of complex **1** with $B(C_6F_5)_3$ in the presence of 1-hexene are described. Attempts to characterize a stoichiometric Hf−C_{Aryl} insertion by using chelating olefins, 2-vinylpyridine or 3-ethoxy-1-propylene,[16] are also detailed. In addition, 1-butene is generated in close proximity to each metal center by activation of the $\{N^-,N,C_{Aryl}^-\}$-Hf(n-Bu)$_2$ precursor with $[CPh_3][B(C_6F_5)_4]$, which abstracts a β-H[17] from one n-Bu group. Where possible, the assistance of molecular modeling is used to predict and explain results.

Results and Discussion

***In Situ* Generation and Characterization of the Aryl Monoinserted Species.** Several activation reactions of the precatalyst **1** with $B(C_6F_5)_3$ in the presence of a small excess of 1-hexene (3−6 equiv) were carried out under different experimental conditions (different temperature, solvent, order of addition of reagents, etc.) within an NMR tube. In all cases, resonances typical of poly(1-hexene) appear in the ^{1}H NMR spectrum without any appreciable variation of the resonances due to the ion pair **2**, which forms as a consequence of methyl abstraction by $B(C_6F_5)_3$ (Supporting Information). These data suggest that the rate of initiation is much lower than propagation, and consequently, a small fraction of active sites are responsible for the observed polymerization.[18,19]

On the contrary, when precatalyst **1** is activated with $B(C_6F_5)_3$ in the presence of a large excess of 1-hexene (170 equiv) at low temperature (−56 °C), a new set of resonances is observed in the ^{1}H NMR spectrum (Figures 4S−7S, Supporting Information) in addition to those of poly(1-hexene) (polymerization was complete in about 50 min). A detailed multinuclear and multidimensional NMR study indicates the new set of resonances is due to the aryl monoinserted species **3** shown in Scheme 3. A

Scheme 3. Activation of 1 with $B(C_6F_5)_3$ in the Presence of an Excess of 1-Hexene[a]

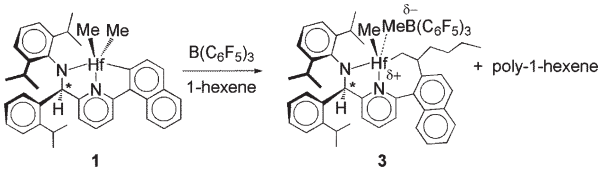

[a] The stereoisomer with *R*-configuration at C* is shown, although a racemic mixture was used.

complete assignment of ^{1}H and ^{13}C NMR resonances of **3** is carried out starting from the singlet at 6.16 ppm in the ^{1}H NMR spectrum, which in this family of compounds corresponds to H17 (Figure 1A),[10] following the scalar and dipolar connectivity in the ^{1}H−COSY, ^{1}H,^{13}C-HMQC, ^{1}H,^{13}C-HMBC, and ^{1}H-NOESY experiments, respectively. Considering the importance of characterization of monoinserted species **3**, some details of the NMR assignments are highlighted here, especially those protons essential for elucidating the three-dimensional structure of **3**.

The *first key point* is the assignment of the three broad septets corresponding to H24, H31, and H34 due to the CH moieties of the three isopropyl groups. H31 is distinguished from H24 and H34 by the lack of an NOE interaction with H17 (Figure 1B). The discrimination between H24 and H34 is possible considering that the former is scalarly coupled with H24a (Figure 1D), which is easily assigned due to its NOE interaction with H14 (Figure 1B). A *second key point* concerns discrimination between H2 and H3 aromatic resonances, which is complicated by the partial overlap with the doublet of H5. H2 is identified by a weak long-range heteronuclear correlation with a carbon resonance at 48 ppm consequently assigned to C_b (Figure 1C). The resonances corresponding to C_b and C_a (δ_C = 78 ppm) are in reasonable agreement with those observed previously in experiments using $^{13}CH_2{=}^{13}CH_2$.[9] Finally, resonances corresponding to the Hf-Me group (C38) are found at δ_H = 0.06 ppm and δ_C = 60.6 ppm.

The ^{13}C-JMOD NMR spectrum allows assignment of the *regiochemistry of the migratory insertion*. In fact, it demonstrates that C_a and C_b are secondary and tertiary carbons, respectively, thus revealing that a 1,2-insertion of 1-hexene occurs into the Hf−C_{Aryl} bond. As far as the *stereochemistry of the migratory insertion* is concerned, the observation of a strong NOE contact between H_b and H2 (Figure 1B) indicates that the *re*-enantioface is selected by the catalyst having an *R*-configuration at the bridging carbon (and conversely the *si*-enantioface by the *S*-one). Consequently, the butyl chain in the β-position is oriented back toward the

(16) Bijpost, E. A.; Zuideveld, M. A.; Meetsma, A.; Teuben, J. H. *J. Organomet. Chem.* **1998**, *551*, 159. For a more recent paper describing the use of 3-(methylthio)-1-propylene for similar studies see: Richter, B.; Meetsma, A.; Hessen, B.; Teuben, J. H. *Angew. Chem., Int. Ed.* **2002**, *41*, 2166.

(17) (a) Lian, B.; Toupet, L.; Carpentier, J.-F. *Chem.—Eur. J.* **2004**, *10*, 4310. (b) Mehrkhodavandi, P.; Schrock, R. R. *J. Am. Chem. Soc.* **2001**, *123*, 10746. (c) Bochmann, M.; Sarsfield, M. J. *Organometallics* **1998**, *17*, 5908. (d) Jerkunica, J. M.; Traylor, T. G. *J. Am. Chem. Soc.* **1971**, *93*, 6278. (e) Hannon, J. S.; Traylor, T. G. *J. Org. Chem.* **1981**, *46*, 3645.

(18) (a) Landis, C. R.; Rosaaen, K. A.; Sillars, D. R. *J. Am. Chem. Soc.* **2003**, *125*, 1710. (b) Klamo, S. B.; Wendt, O. F.; Henling, L. M.; Day, M. W.; Bercaw, J. E. *Organometallics* **2007**, *26*, 3018.

(19) Mehrkhodavandi, P.; Bonitatebus, P. J.; Schrock, R. R. *J. Am. Chem. Soc.* **2000**, *122*, 7841.

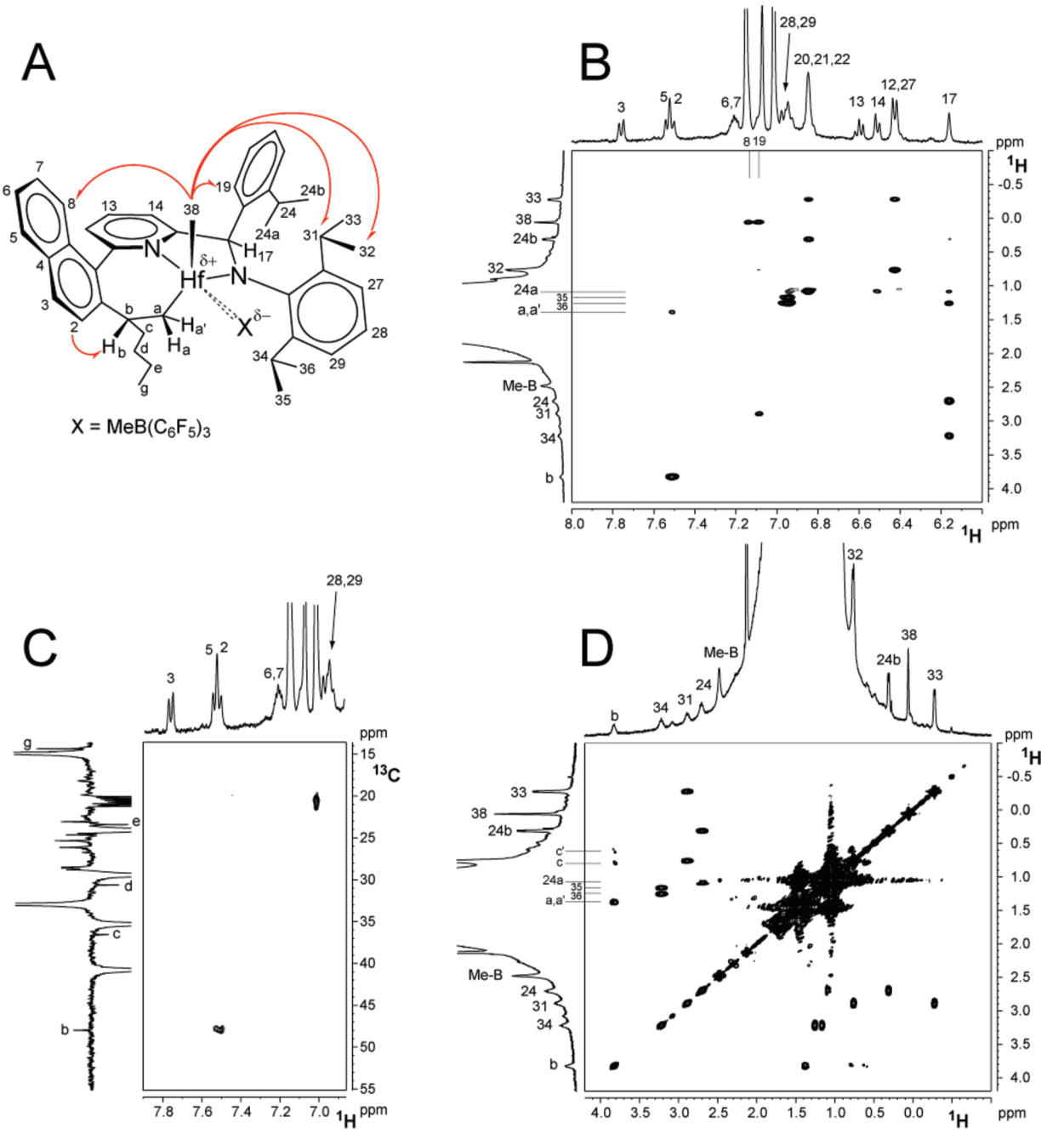

Figure 1. NMR characterization of the monoinserted product **3**, including (A) a molecular sketch of ion pair **3** with red arrows indicating relevant NOEs; (B) a section of the ^{1}H-NOESY NMR spectrum of **3**; (C) a section of the ^{1}H,^{13}C-HMBC NMR spectrum of **3** showing the long-range correlation between H2 and C_b; (D) a section of the ^{1}H−COSY NMR spectrum of **3**.

pyridine ring of the ligand (Figure 1A). The strong interactions observed in the ^{1}H-NOESY spectrum between H38 and H19, H31, and H32 (Figures 1B and S15) show that the *stereochemistry at the metal* remains the same as that of the starting ion pair **2**, with the terminal methyl group oriented on the opposite side with respect to H17.[10] The presence of the C_a−C_b bridge introduces some flexibility, allowing the naphthyl ring to release the eclipsing interaction with the backbone of the pyridine ring present in **2**;[10] consistently, H8 is found spatially close to H38, as indicated by the observation of a strong contact between them in the ^{1}H NOESY spectrum (Figure 1B). A previous work[9] had determined the solid state structure of the ligand residue of a quenched catalyst during a 4-methyl-1-pentene homopolymerization. While the chirality of the metal center was lost, the assignment of the remaining two stereocenters agrees with the assigned structure in Figure 1A.

Finally, the *structure of the ion pair* **3** is determined. The chemical shift difference between *p*-F and *m*-F resonances ($\Delta_{m\text{-F},p\text{-F}}$ = 4.64 ppm)[20] of the counterion indicates that **3** is present in solution as an inner-sphere ion pair[21] where the methyl group of the anion steadily points toward the metal center. In full agreement, the ^{19}F,^{1}H HOESY NMR spectra

(20) The value of $\Delta(m,p\text{-F})$ (^{19}F NMR) is a good probe of the coordination of $MeB(C_6F_5)_3^-$ at cationic d^0 metals. Horton, A. D.; de With, J. *Organometallics* **1997**, *16*, 5424, and references therein.

(21) Macchioni, A. *Chem. Rev.* **2005**, *105*, 2039.

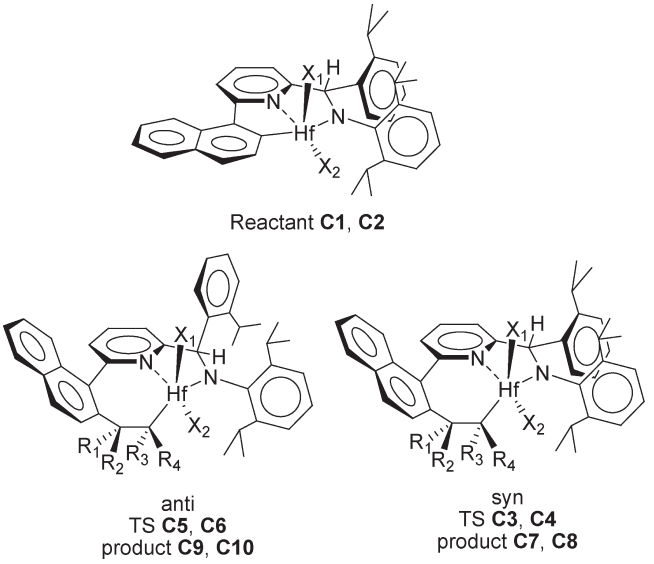

Figure 2. Reactant species and transition states/products that can be formed from insertion of an olefin into the Hf−$C_{Naphthyl}$ bond.

show interionic contacts between the *o*-F nuclei and some resonances of the cation that are much stronger than those due to *m*-F and *p*-F nuclei.[22] Specifically, the anion preferentially interacts with H38, H_a, H_a, and H32 and, more weakly, with H35, H31, H_b, H2, H27, H28, and H29 (Supporting Information).

It is worth noting that the monoinserted ion pair **3** is intercepted under catalytic conditions, and its formation occurs on a time scale comparable with that of olefin enchainment. Interestingly, **3** has an intact Hf-Me moiety, indicating that a single olefin insertion occurs exclusively into the Hf−C_{Aryl} bond. An *a posteriori* inspection shows that **3** is already present before complete 1-hexene consumption even in the first spectrum recorded approximately 2 min after the addition of $B(C_6F_5)_3$ (Figure 2S, Supporting Information). On the other hand, organometallic species bearing a polymeryl chain are never observed under these conditions. This suggests that either initiation of **3** (a **BI**-like species) to give species **BII** is much slower than subsequent propagation (Scheme 4) or, alternatively, **3** is an "out of cycle" species and is irrelevant to catalysis.

Computational Probe of Selectivity of First Olefin Insertion. Computationally, we chose to examine insertions into the Hf−C_{Aryl} bond using density functional theory (DFT). Previous calculations indicated that these reactions proceed with 1,2-regioselectivity, stereoselectivity directs the substituent toward the pyridine, and the facial selectivity occurs from the same side as the isopropylphenyl (^{i}PrPh).[9] While the regio- and stereochemistries agree with the experimental assignment of the inserted species, the facial selectivity does not. We therefore revisited the calculations including the borane activator $\{B(C_6F_5)_3\}$ to determine its role in the Hf−C_{Aryl} insertion process.

Figure 2 shows possible insertion modes with the syn and anti species drawn to indicate the relative positions of the

Scheme 4. Possible Initiation and Propagation Starting from the Aryl-Monoinserted Species BI

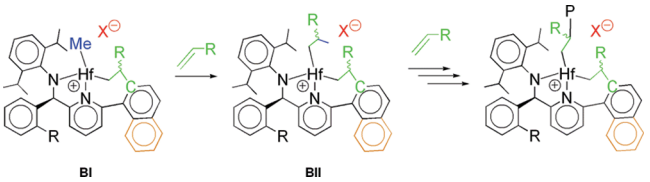

^{i}PrPh and inserted olefin. The stereo- and regiochemistry depend on whether the methyl is located on R_1−R_4. The addition of the counterion to the calculations adds another level of complexity, as X_1 and X_2 can be Me or $MeB(C_6F_5)_3^-$. If $X_1 = MeB(C_6F_5)_3^-$, then the anion is opposite or trans to the inserted olefin, while if $X_2 = MeB(C_6F_5)_3^-$, then the anion is adjacent to the inserted olefin.

Table 1 collects the data on the reactant (**C1**, **C2**) species, the transition states (TSs) (**C3**−**C6**), and the products (**C7**−**C10**) of ethylene and propylene insertions.[23] The data are enthalpies relative to the lowest energy uninserted species, **2**. The data without the counterion are also included in the table as the lower set of entries (note that there are only half as many structures since X_1 = Me and X_2 is the open coordination site). There is a large difference in the scales with and without counterion; with the anion, the barriers are realistic values for enthalpies of activation, but without a counterion, the reactions are too exothermic and the barriers too low. However, in both cases, the different TSs can be compared to predict the selectivity, while with the anion, the barrier to activation can also be estimated qualitatively.

The first thing to observe is that, regardless of whether anions are included, insertions are always faster for ethylene (**e**) than propylene. Since our focus is on the selectivity of α-olefin insertion, we shall not discuss ethylene insertions any further. As observed from the data with no counterion, insertions are favored syn, i.e., on the same face as the ^{i}PrPh group, as the lowest energy TS is **C4a**. The next lowest energy TSs are **C4b** and **C6a**. These results agree with previous computational work focused on a comparison of insertions into the Hf−C_{Aryl} and Hf−C_{Me} bonds.[9] However, this result is inconsistent with the species assigned by NMR from the previous section. The structure **C6a** corresponds to the experimentally determined one, despite the fact that it resides 3.5 kcal/mol above **C4a**.

Following this inconsistency, the calculations were extended to include the anion. It appears that the counterion prefers to reside adjacent to the inserting moiety, position X_2, in agreement with its experimentally determined position in both the reactant[10] and product. When the anion is included, the facial selectivity changes, and **C6a** is the lowest energy TS, in agreement with the experimentally identified isomer. The next lowest energy structures, **C5b** and **C6b**, correspond to 1,2-insertions on the same face, only with opposite stereochemistry (the anion is in the two different positions). These TSs are less than 1 kcal/mol above **C6a**. Even if the position of the anion is ignored, all four 1,2-insertions on both faces lie within 2.3 kcal/mol of **C6a**. The lowest 2,1-inserted TS (**C6c**) is only 4.3 kcal/mol higher in energy. While the computations and experiments agree on the most likely species, it is clear that a myriad of different diastereomers

(22) (a) Zuccaccia, C.; Stahl, N. G.; Macchioni, A.; Chen, M. C.; Roberts, J. A.; Marks, T. J. *J. Am. Chem. Soc.* **2004**, *126*, 1448. (b) Song, F.; Lancaster, S. J.; Cannon, R. D.; Schormann, M.; Humphrey, S. M.; Zuccaccia, C.; Macchioni, A.; Bochmann, M. *Organometallics* **2005**, *24*, 1315.

(23) Computational structures are labeled with the prefix **C**.

Table 1. DFT Energies (kcal/mol) Relative to the Reactants (C1, C2) of the TSs (C3−C6) and Products (C7-C10) for Ethylene (e) and Propylene (a−d) Insertion into the Hf−C_{Aryl} Bond with $MeB(C_6F_5)_3^-$ Anion and without Anion[a]

	TS syn		TS anti		product syn		product anti	
	C3	**C4**	**C5**	**C6**	**C7**	**C8**	**C9**	**C10**
R_1 = Me, R_{2-4} = H (a)								
X_1 = $MeB(C_6F_5)_3^-$, X_2 = Me	21.2		25.3		−1.2		−8.4	
X_1 = Me, X_2 = $MeB(C_6F_5)_3^-$		20.4		19.0		−9.9		−9.6
X_1 = Me, X_2 = vacancy		−6.8		−3.3		−25.2		−22.7
R_2 = Me, $R_{1,3-4}$ = H (b)								
X_1 = $MeB(C_6F_5)_3^-$, X_2 = Me	22.6		19.7		−4.7		−11.8	
X_1 = Me, X_2 = $MeB(C_6F_5)_3^-$		21.3		20.0		−13.9		−13.0
X_1 = Me, X_2 = vacancy		−5.2		−1.7		−29.2		−26.8
R_3 = Me, $R_{1-2,4}$ = H (c)								
X_1 = $MeB(C_6F_5)_3^-$, X_2 = Me	30.7		40.0		−5.3		−8.6	
X_1 = Me, X_2 = $MeB(C_6F_5)_3^-$		27.2		23.3		−11.6		−9.7
X_1 = Me, X_2 = vacancy		1.4		4.9		−27.4		−20.4
R_4 = Me, R_{1-3} = H (d)								
X_1 = $MeB(C_6F_5)_3^-$, X_2 = Me	25.6		26.2		2.0		−8.4	
X_1 = Me, X_2 = $MeB(C_6F_5)_3^-$		27.9		24.9		−8.0		−3.6
X_1 = Me, X_2 = vacancy		−2.7		−0.1		−26.8		−24.3
R_{1-4} = H (e)								
X_1 = $MeB(C_6F_5)_3^-$, X_2 = Me	18.7		22.6		−9.5		−17.3	
X_1 = Me, X_2 = $MeB(C_6F_5)_3^-$		17.0		15.4		−18.4		−17.8
X_1 = Me, X_2 = vacancy		−7.7		−4.3		−33.5		−27.9

[a] See Figure 2 for the structures.

could be formed. In addition, the enthalpic barrier for propylene insertion (**C6a**) is 19.0 kcal/mol, suggesting slow activation.

The product energies are also collected in Table 1. A very interesting result is that the kinetically favored product, **C10a** (from TS **C6a**), is not nearly the most stable thermodynamic species. In fact, even if the position of the anion is ignored, five of the eight other diastereomers are more stable, including two different 2,1-inserted species, **C8c** and **C10c**. The favored kinetic product, **C10a**, is 4.3 kcal/mol less stable than **C8b**, which is the most stable product.

Trapping the Monoinserted Species by Means of Chelating Olefins. Although the above reactions directly demonstrate the ability for α-olefin insertion into the Hf−C_{Aryl} bond of **2**, quantitative generation of a monoinsertion product is hindered by polymer formation. In order to explore the scope of olefin insertion into the Hf−C_{Aryl} bond and, at the same time, avoid polymer formation, we turned our investigation to stoichiometric reactions of heteroatom-containing olefins that should prevent multiple insertions due to chelation effects. This strategy has been successfully applied by Teuben and co-workers in migratory insertion of 3-ethoxy-1-propylene into the Zr−Me bond of $[(\eta^5\text{-}C_5Me_5)_2ZrMe][MeB(C_6F_5)_3]$, leading to a single 1,2-insertion with formation of an oxygen-stabilized cationic zirconacyclopentane.[16] Results of reactions of **2** with both 3-ethoxy-1-propylene and 2-vinylpyridine as chelating olefins are described below.

Computationally, we examined olefin insertions into the simplified achiral catalyst (no isopropylphenyl group) with no counterion. The goal was to understand the stabilization gained by the chelate to see if insertion into the Hf−C_{Aryl} bond is predicted. The relative energies of the six transition states for olefin insertion into the Hf−C_{Aryl} and Hf−C_{Me} bond are collected in Table 2 for propylene (**C11**), 4-vinylpyridine (**C12**), 2-vinylpyridine (**C13**), and 3-ethoxy-1-propylene (**C14**). For the simple α-olefin, propylene, insertions are favored into the Hf−C_{Aryl} bond in a 1,2-fashion (**C11a**). However, the substrates 2-vinylpyridine and 3-ethoxy-1-propylene preferentially insert in a 2,1-fashion, maximizing interactions with the metal. The calculations suggest that for these latter two substrates insertions into the Hf−C_{Aryl} bond (**C13d**, **C14d**) are preferred over the those into the Hf−C_{Me} bond (**C13g**, **C14g**), although both produce substantially more stable products than 1,2-insertions. These results suggest that the use of a chelating olefinic substrate could trap an aryl-inserted monomer in a stoichiometric reaction.

Scheme 5. Species Derived from the Reaction of 2 with 3-Ethoxy-1-propylene[a]

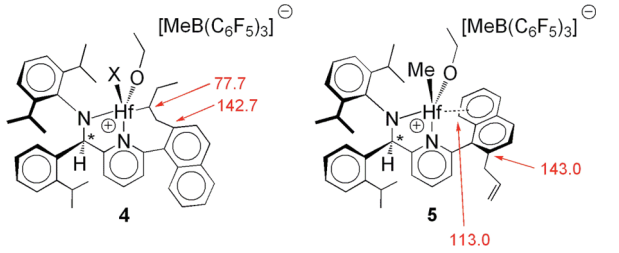

[a] X is a molecule of 3-ethoxy-1-propylene coordinated at the metal as a neutral ligand through the oxygen atom. Values of δ (ppm) for selected ^{13}C resonances are shown in red. The stereoisomer with *R*-configuration at C* is shown, although a racemic mixture was used.

(**a**) **3-Ethoxy-1-propylene.** The reaction of **2** with a stoichiometric amount of 3-ethoxy-1-propylene (EOP) turned out to be more complicated than expected, producing a mixture of species under all examined experimental conditions. Despite the complicated product mixture, it is clear that a fast and complete anion displacement from the first coordination sphere occurs, since the ^{19}F NMR spectrum shows a single set of sharp resonances corresponding to a noncoordinated $MeB(C_6F_5)_3^-$ anion ($\Delta_{m\text{-}F,p\text{-}F}$ = 2.42 ppm).[20] On the contrary, the ^1H NMR spectrum shows rather broad resonances with several singlets in the Hf-Me region. Addition of a small excess of 3-ethoxy-1-propylene (2−3 equiv) leads to separation of an oil from the solution. NMR investigation of this oil (Supporting Information) reveals that a mixture of two products is formed in approximately a 70:30 molar ratio; the structure of the major component of this oil is assigned to the ion pair **4** (Scheme 5). A sample enriched (ca. 50−60% of the mixture) in the other species

Scheme 6. Postulated Pathway for Reaction of 2 with 3-Ethoxy-1-propylene Leading to the Formation of 4 and 5[a]

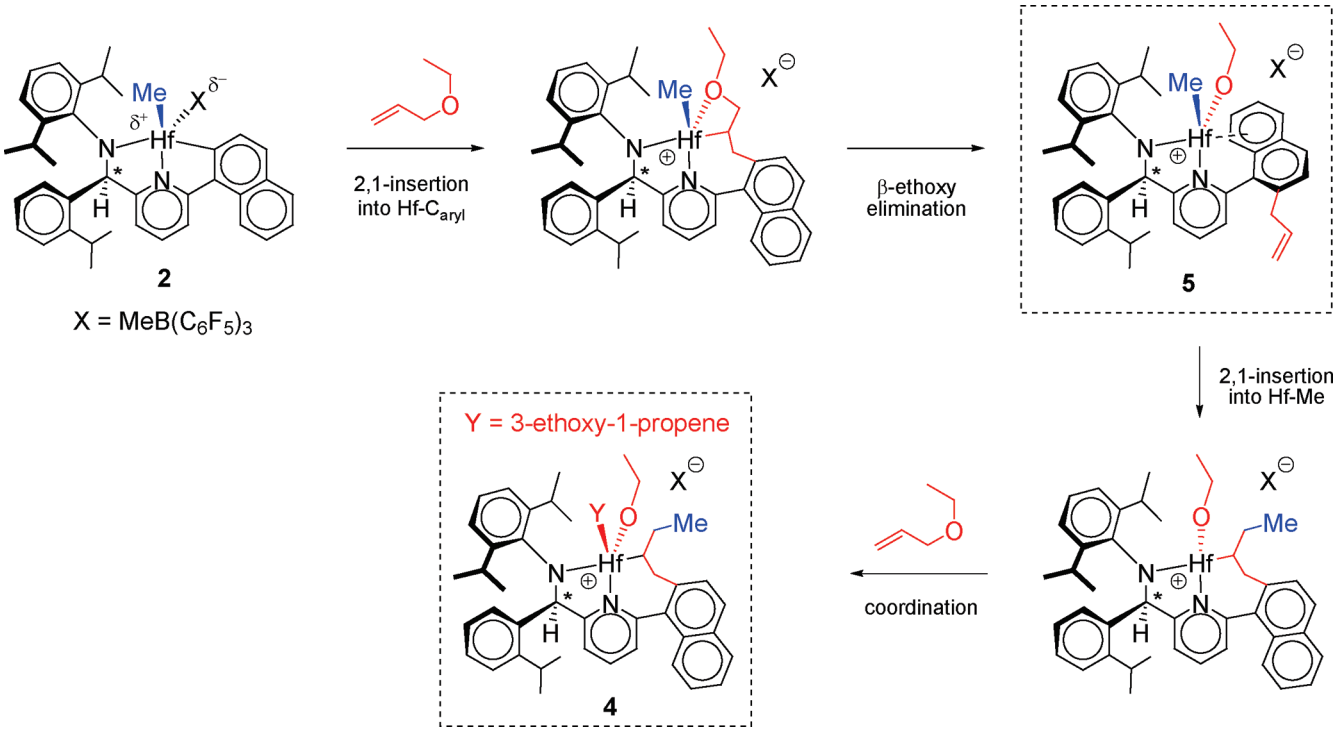

[a] X is the $MeB(C_6F_5)_3$ anion, and Y is a molecule of 3-ethoxy-1-propylene coordinated at the metal as a neutral ligand through the oxygen atom.

Table 2. DFT Energies of Six TSs Relative to the 1,2-Aryl Insertion Species, a, for Four Different Monomers[a]

substrate	1,2-aryl, **a**	1,2-aryl, **b**	2,1-aryl, **c**	2,1-aryl, **d**	1,2-Me, **f**	2,1-Me, **g**
propylene **C11**	0.0	1.9	6.9	3.7	7.0	11.2
4-vinylpyridine **C12**	0.0	2.6	4.5	2.6	8.7	7.8
2-vinylpyridine **C13**	0.0	3.3	3.6	−17.0	11.1	−7.9
3-ethoxy-1-propylene **C14**	0.0	1.7	2.5	−16.0	9.1	−7.9

[a] Only insertions into the $Hf-C_{Me}$ with the olefinic substituent directed away from the DIP were examined. The structures of the $Hf-C_{Aryl}$ insertion species (**a**−**d**) correspond to that in Figure 2.

was obtained when **2** was reacted with a smaller excess of 3-ethoxy-1-propylene. Although complete assignment was strongly hampered by extensive overlapping, NMR spectra (Supporting Information) suggest the molecular structure **5** shown in Scheme 5.

Evidently, the reactivity of the ion pair **2** with EOP is much more complex than that of $[(\eta^5\text{-}C_5Me_5)_2ZrMe][MeB(C_6F_5)_3]$[16] and involves a C−O bond cleavage. Three different mechanisms were proposed to explain the formation of **4** and **5**, and a thorough computational study was performed to provide insight into the likely path. Two possibilities begin with a first insertion of EOP into either the $Hf-C_{Me}$[24] or $Hf-C_{Aryl}$ bonds, while the third involves a concerted route to arrive at **5** directly through breaking the $Hf-C_{naphthyl}$ bond.[25] Complete computational details and a thorough discussion of the differences in these three pathways are given in the Supporting Information. Overall, the evidence overwhelmingly suggests that the reaction proceeds as shown in Scheme 6 through a 2,1-insertion of EOP into the $Hf-C_{Aryl}$ bond, β-ethoxy elimination, and reinsertion of the propenyl group into the $Hf-C_{Me}$ bond.

Scheme 7. Reaction of Ion Pair 2 with 2-Vinylpyridine[a]

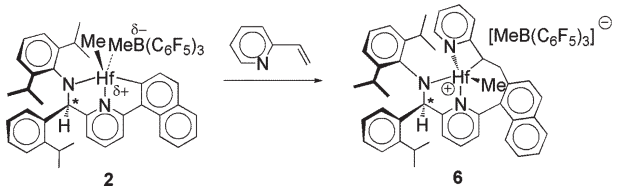

[a] The stereoisomer with *R*-configuration at C* is shown although a racemic mixture was used.

(**b**) **2-Vinylpyridine.** In order to avoid complications due to C-heteroatom activation, we decided to use a substituted α-olefin in which the donor atom is incorporated into a more robust aromatic ring. The reaction of **2** with 2-vinylpyridine leads to the prevalent (80−90%) formation of the ion pair **6** (Scheme 7) through a 2,1-insertion of the olefin into the $Hf-C_{Aryl}$ bond. The structural assignment was ascertained by the absence of resonances around 200 ppm in the ^{13}C NMR spectrum, where the naphthyl cyclometalated carbon resonance falls,[10] and by the $^1H,^{13}C$-HMBC NMR experiment that establishes the connection $C_i-C39-C40-C1$ (Figure 3). The *regiochemistry of the insertion* is again determined by the ^{13}C-JMOD NMR spectrum; C39 and C40 are found to be

(24) Komiya, S.; Srivastava, R. S.; Yamamoto, A.; Yamamoto, T. *Organometallics* **1985**, *4*, 1504, and references therein.

(25) (a) Cheung, M. S.; Chan, H.-S.; Xie, Z. *Organometallics* **2005**, *24*, 5217. (b) Trifonov, A. A.; Spaniol, T. P.; Okuda, J. *Dalton Trans.* **2004**, 2245. (c) van der Boom, M. E.; Liou, S.-Y.; Ben-David, Y.; Shimon, L. J. W.; Milstein, D. *J. Am. Chem. Soc.* **1998**, *120*, 6531. (d) Deelman, B.-J.; Booij, M.; Meetsma, A.; Teuben, J. H.; Kooijman, H.; Spek, A. L. *Organometallics* **1995**, *14*, 2306, and references therein.

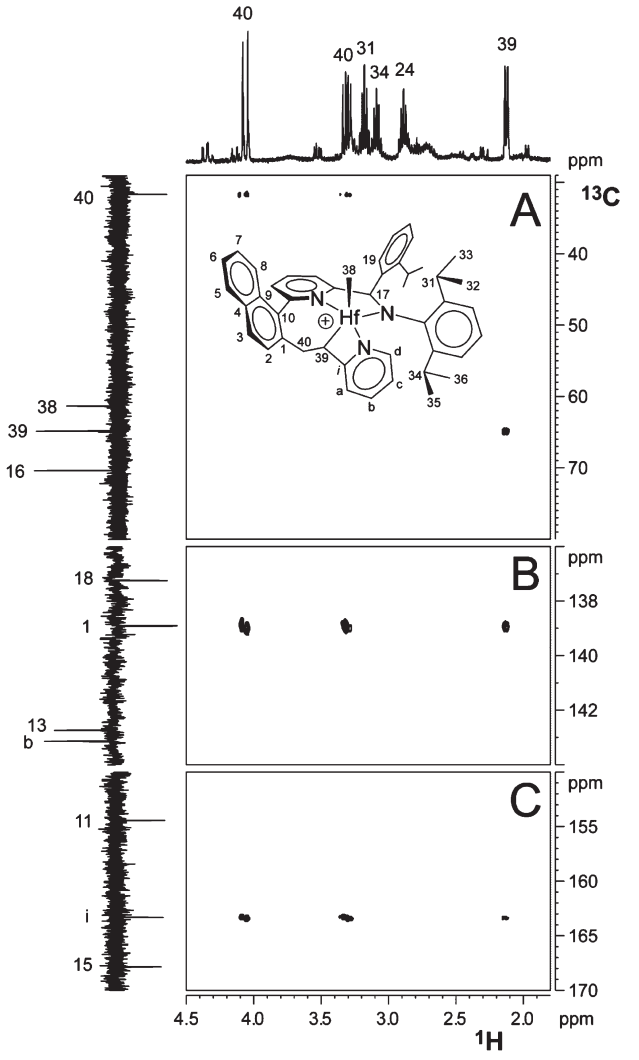

Figure 3. Three sections of the $^{1}H,^{13}C$ HMQC (A) and $^{1}H,^{13}C$ HMBC (B and C) NMR spectra of complexes **6** (C_6D_5Cl, 298 K), demonstrating the connection C_i−C39−C40−C1.

tertiary and secondary carbons, respectively. These data are all consistent with a 2,1-insertion, which is typically observed for aromatic olefins.[26,27] The ^{19}F NMR spectrum shows a single set of resonances corresponding to an outer-sphere $MeB(C_6F_5)_3^-$ anion,[20] strongly suggesting coordination of the nitrogen of 2-vinylpyridine to the metal center.

The three-dimensional structure of **6** in solution is determined through ^{1}H−NOESY spectroscopy (Figure 4). The strong interactions of H38 with H19, H31 and H32 (Figure 4A and C) indicate that the *stereochemistry at the metal* is the same as the starting ion pair **2**,[10] with the terminal methyl group oriented on the opposite side with respect to H17. Concerning the *olefin insertion stereochemistry*, the strong NOE contacts between H39 and both H34 and H35 (Figure 4D), as well as the absence of any appreciable interaction between H38 and H39, strongly support a selection of the *re*-enantioface.[28] The close proximity of $H40_{eq}$ and H2 (Figure 4B) also provides a hint for 2,1-regiochemistry. The $^{3}J_{HH}$ coupling constant between H39 and $H40_{ax}$ amounts to 8.1 Hz, while the corresponding constant between H39 and $H40_{eq}$ is below the experimental detectability (< 1 Hz). According to the Karplus relationship, these values suggest a quasi-eclipsed conformation (Figure 5). In agreement with this steric arrangement, $H40_{ax}$ rather than $H40_{eq}$ shows an intense NOE interaction with H39. Coordination of the inserted olefin through the pyridine nitrogen is further supported by the NOE cross-peak between H38 and H_d (Figure 4A). Again, the presence of the C39−C40 bridge introduces some flexibility to release the eclipsing interaction with the backbone pyridine;[10] as a consequence, H8 is found spatially close to H38 (Figure 4A).

Although complete characterization of the two byproducts accounting for 10−20% of the product mixture is impossible, resonances around $\delta_H = -1.2$ ppm typical of the Hf−C_{Me} moiety are present (Figure 29S, Supporting Information). NMR evidence for olefin insertion into the Hf−C_{Me} bond is not observed in this reaction, suggesting that the first insertion of 2-vinylpyridine proceeds *quantitatively into the Hf−C_{Aryl} bond.*

Following characterization of ion pair **6**, the possibility that this species may itself catalyze α-olefin polymerizations was investigated. This species shows no reaction with 1-hexene, probably a consequence of N-pyridine coordination to hafnium. Reactivity is observed upon addition of a stoichiometric amount of 2-vinylpyridine, leading to complete consumption of **6** with formation of ion pair **7**[29] and evolution of methane (Scheme 8). In **7**, the olefinic carbon directly bonded to the hafnium resonates at $\delta_C = 211$ ppm, in agreement with the literature.[26] The coupling constant of the olefinic protons (ca. 15 Hz) indicates a trans geometry around the double bond. As in **6**, the ^{19}F NMR spectrum shows a single set of resonances corresponding to an outer-sphere $MeB(C_6F_5)_3^-$ anion.[20] Considering the trans geometry of the double bond, it seems more plausible that the N-pyridine atom of the inserted olefin coordinates at the metal center, pushing the anion to the outer coordination sphere. As in other cases, NOE studies establish that the CH moiety directly bonded to hafnium is positioned in a pseudo-trans position with respect to H17. Similar C(sp^2)−H bond activations of 2-vinylpyridine have been observed for a number of metal complexes,[30] but to our knowledge, these examples are all cyclometalations

(26) Guram, A. S.; Jordan, R. F. *Organometallics* **1991**, *11*, 3470.
(27) Correa, A.; Galdi, N.; Izzo, L.; Cavallo, L.; Oliva, L. *Organometallics* **2008**, *27*, 1028, and references therein.
(28) The *si*-enantioface is consequently selected when the isomer with the *S*-configuration at the bridging amine-pyridyl carbon is considered.

(29) A similar alkyl-displacement reaction has been recently reported by Esteruelas and co-workers for osmium and ruthenium derivatives: Buil, M. L.; Esteruelas, M. A.; Goni, E.; Olivan, M.; Onate, E. *Organometallics* **2006**, *25*, 3076, and references therein.
(30) (a) Foot, R.; Heaton, B. T. *J. Chem. Soc., Chem. Commun.* **1973**, 838. (b) Bruce, M. I.; Goodall, B. L.; Matsuda, I. *Aust. J. Chem.* **1975**, *28*, 1259. (c) Foot, R.; Heaton, B. T. *J. Chem. Soc., Dalton Trans.* **1979**, 295. (d) Burgess, K.; Holden, H. D.; Johnson, B. F. G.; Lewis, J.; Hursthouse, M. B.; Walker, N. P. C.; Deeming, A. J.; Manning, P. J.; Peters, R. *J. Chem. Soc., Dalton Trans.* **1985**, 85. (e) Newkome, G. R.; Theriot, K. J.; Cheskin, B. K.; Evans, D. W.; Baker, G. R. *Organometallics* **1990**, *9*, 1375. (f) Jia, G.; Meek, D. W.; Gallucci, J. C. *Organometallics* **1990**, *9*, 2549. (g) Wong, W.-Y.; Wong, W.-T. *J. Organomet. Chem.* **1996**, *513*, 27. (h) Wong-Foy, A. G.; Henling, L. M.; Day, M.; Labinger, J. A.; Bercaw, J. E. *J. Mol. Catal. A: Chem.* **2002**, *189*, 3. (i) Lau, J. P.-K.; Wong, W.-T. *Inorg. Chem. Commun.* **2003**, *6*, 174. (j) Müller, J.; Hirsch, C.; Ha, K. *Z. Anorg. Allg. Chem.* **2003**, *629*, 2180. (k) Navarro, J.; Sola, E.; Martín, M.; Dobrinovitch, I. T.; Lahoz, F. J.; Oro, L. A. *Organometallics* **2004**, *23*, 1908. (l) Ozerov, O. V.; Pink, M.; Watson, L. A.; Caulton, K. G. *J. Am. Chem. Soc.* **2004**, *126*, 2105. (m) Eguillor, B.; Esteruelas, M. A.; Oliván, M.; Oñate, E. *Organometallics* **2005**, *24*, 1428. (n) Esteruelas, M. A.; Fernández-Alvarez, F. J.; Oliván, M.; Oñate, E. *J. Am. Chem. Soc.* **2006**, *128*, 4596. (o) Buil, M. L.; Esteruelas, M. A.; Goni, E.; Oliván, M.; Oñate, E. *Organometallics* **2006**, *25*, 3076. (p) Azam, K. A.; Bennett, D. W.; Hassan, M. R.; Haworth, D. T.; Hogarth, G.; Kabir, S. E.; Lindeman, S. V.; Salassa, L.; Simi, S. R.; Siddiquee, T. A. *Organometallics* **2008**, *27*, 5163.

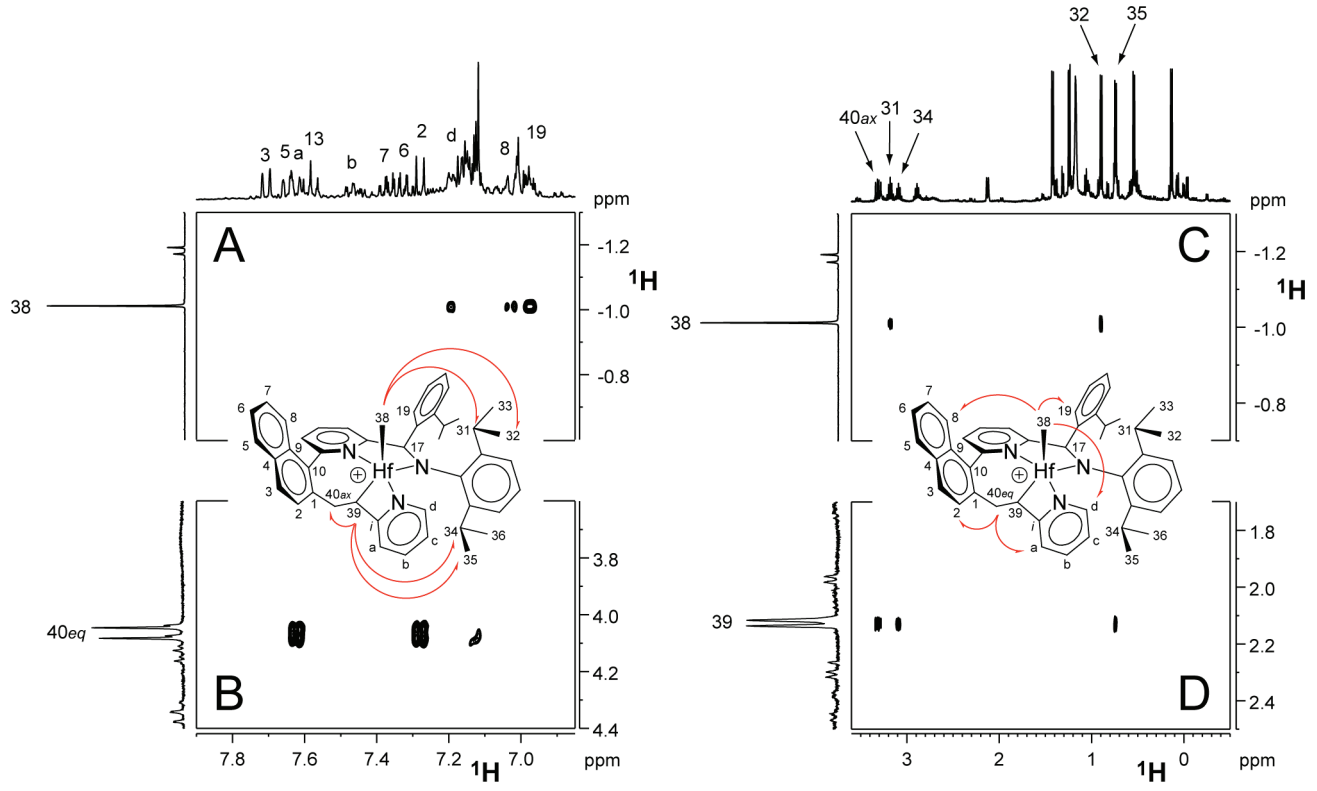

Figure 4. Four sections of the ^{1}H-NOESY NMR spectrum of complex **6** (C_6D_5Cl, 298 K).

Scheme 8. Reaction of Ion Pair 6 with 2-Vinylpyridine[a]

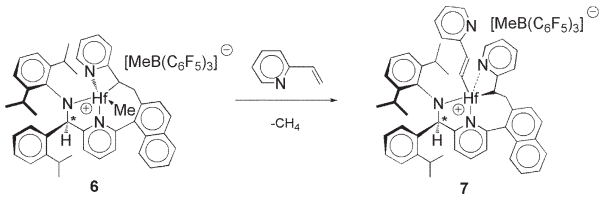

[a] The stereoisomer with *R*-configuration at C* is shown although a racemic mixture was used.

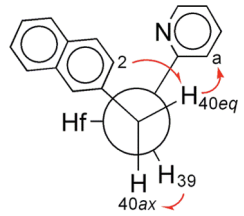

Figure 5. Newmann projection of complex **6** along the C40−C39 bond. Red arrows indicate the observed NOE interactions.

facilitated by chelation of the pyridine nitrogen.[31] The trans configuration of the double bond indicates that this C−H activation process proceeds without chelation assistance.

Activation of $\{N^-,N,C_{Aryl}^-\}Hf(n\text{-}Bu)_2$ (8) with $[CPh_3][B(C_6F_5)_4]$. The results discussed above clearly suggest that the first insertion of olefin preferentially occurs into the Hf−C_{Aryl} bond even under catalytic conditions, resulting in formation of a **BI**-type species with potential catalytic activity. At the same time, these data do not exclude that the aryl cyclometalated ion pair **2** could also be an active catalyst.

In order to perform a more stringent competitive experiment between these two species, we decided to investigate the activation of the dibutyl analogue of **1** with $[CPh_3][B(C_6F_5)_4]$. Dialkyl complexes of group IV metals bearing alkyl substituents with one or more β-hydrogens are not typically thermally robust,[32] but several examples of stable group IV dibutyl complexes have been reported.[17,33] The motivation for this experiment centers around the possibility of generating a single molecule of 1-butene in close proximity to each $[\{N^-,N,C_{Aryl}^-\}Hf(n\text{-}Bu)][B(C_6F_5)_4]$ ion pair through β-H abstraction at one *n*-butyl group (Scheme 9).[17] The experiment is designed to favor pathway A; since the Hf-*n*-Bu species is a better mimic for the propagating Hf-polymeryl species, rates of initiation and propagation

(31) Jun, C.-H.; Moon, C.-W.; Lee, D.-Y. *Chem.—Eur. J.* **2002**, *8*, 2423. and references therein.

(32) (a) Negishi, E.-I.; Takahashi, T. *Acc. Chem. Res.* **1994**, *27* 5, 124, and references therein. (b) Chang, B.-H.; Tung, H.-S.; Brubaker, C. H., Jr. *Inorg. Chim. Acta* **1981**, *51*, 143. (c) McDermott, J. X.; Wilson, M. E.; Whitesides, G. M. *J. Am. Chem. Soc.* **1976**, *98*, 6529. (d) Binger, P.; Müller, P.; Benn, R.; Rufinska, A.; Gabor, B.; Krüger, C.; Betz, P. *Chem. Ber.* **1989**, *122*, 1035. (e) Sinnema, P.-J.; van der Veen, L.; Spek, A. L.; Veldman, N.; Teuben, J. H. *Organometallics* **1997**, *16*, 4245.

(33) For leading examples, see: (a) Paolucci, G.; Pojana, G.; Zanon, J.; Lucchini, V.; Avtomonov, E. *Organometallics* **1997**, *16*, 5312. (b) Amor, F.; Spaniol, T. P.; Okuda, J. *Organometallics* **1997**, *16*, 4765. (c) Amor, F.; Butt, A.; du Plooy, K. E.; Spaniol, T. P.; Okuda, J. *Organometallics* **1998**, *17*, 5836. (d) Mehrkhodavandi, P.; Bonitatebus, P. J., Jr.; Schrock, R. R. *J. Am. Chem. Soc.* **2000**, *122*, 7841. (e) Mehrkhodavandi, P.; Schrock, R. R.; Bonitatebus, P. J. *Organometallics* **2002**, *21*, 5785. (f) Ernst, R. D.; Harvey, B. G.; Arif, A. M. *Z. Kristallogr.-New Cryst. Struct.* **2004**, *219*, 398. (g) Schrock, R. R.; Adamchuk, J.; Ruhland, K.; Lopez, L. P. H. *Organometallics* **2005**, *24*, 857. (h) Boone, H. W.; Coalter, J. N., I. I. I.; Frazier, K. A.; Iverson, C. N.; Munro, I. M.; Vosejpka, P. C. PCT Int. Appl. Publ. No. WO 2007/130307.

Scheme 9. Proposed Pathways for Reaction of 8 with $[CPh_3][B(C_6F_5)_4]$

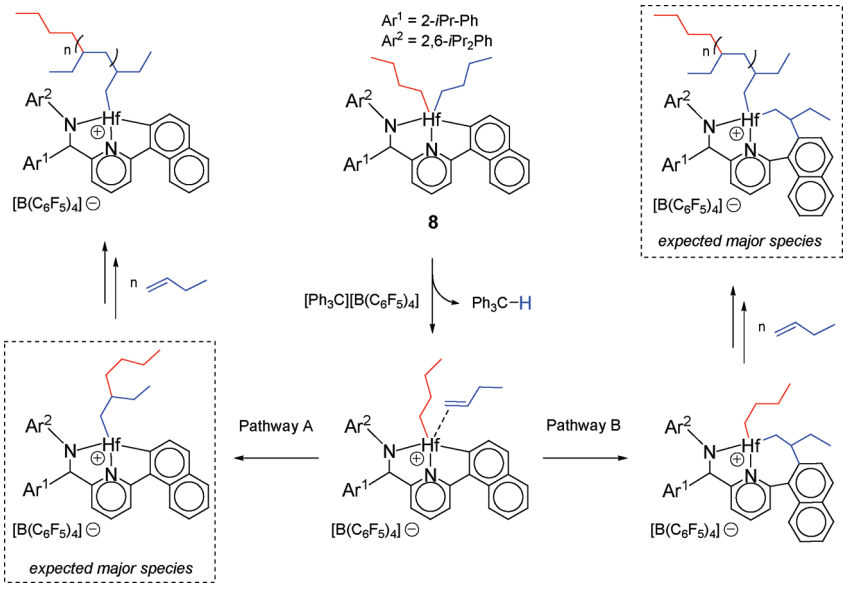

should be competitive. According to the literature,[34−36] this should lead to an increased percentage of active sites and the formation of mainly C_8-dimers, if this path is operative. On the contrary, if pathway B is operative, little difference should be observed with respect to polymerizations conducted with **2** under the assumption that the first insertion into the Hf−C_{Aryl} bond is slow (relative to propagation) and thus limits the formation of the active species.[9] If olefin binding is reversible, this mechanism should result in formation of higher insertion products rather than butene dimers with a product distribution corresponding to the relative rates of insertion into the Hf−C_{Aryl} and Hf−C_{Butyl} bonds.

Reaction of **8** with $[CPh_3][B(C_6F_5)_4]$ in toluene-d_8 at room temperature within an NMR tube results in a quantitative formation of $HCPh_3$ and two diastereoisomeric organometallic species reasonably assignable to [{N$^-$,N, C_{Aryl}^-}Hf(*n*-Bu)][$B(C_6F_5)_4$] **9a** and **9b** ion pairs. *n*-Bu cations of this type are unusual for electrophilic group IV species, as they are susceptible to decomposition via *β*-hydride elimination.[17b,33d,g] However, the stability of **9a**/**b** is not surprising considering the ability of these catalysts to form very high molecular weight polyolefins at high reaction temperatures.[2−5] Decomposition products derived from the transfer of the C_6F_5 moiety(ies) from the counterion to the cation are also observed.[37] Interestingly, no evidence is

Scheme 10. Activation of 8 with $[CPh_3][B(C_6F_5)_4]$[a]

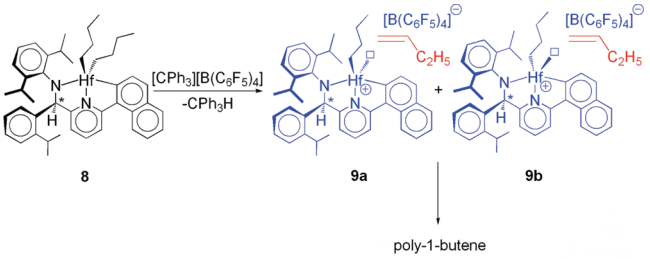

[a] The stereoisomer with *R*-configuration at C* is shown although a racemic mixture was used.

observed for the presence of free/coordinated 1-butene or oligomers formed by insertion(s) of 1-butene into the Hf−C_{Butyl} bond. However, the ^{13}C NMR spectrum of the reaction mixture (acquired during the first 8 h of reaction) instead shows relatively sharp resonances corresponding to poly(1-butene). Integration of the ^{13}C resonances of the polymer with respect to those of $HCPh_3$ indicates that all the liberated 1-butene is polymerized. Consequently, the poly(1-butene) is likely formed on a time scale similar to that of the formation of $HCPh_3$. This is in sharp contrast to the behavior reported by Mehrkhodavandi and Schrock, who observed products from single monomer insertions into Hf−C_{Ethyl} and Hf−$C_{isoPropyl}$ bonds under a similar scheme with diamido pyridine complexes (pathway A in Scheme 9).[17b] Encouraged by this result, we decided to carry out a reaction on a much larger scale in order to isolate and characterize the resulting poly(1-butene) in this unusual "stoichiometric polymerization".

Toward this aim, activation of 2.5 g of **8** with $[CPh_3][B(C_6F_5)_4]$ produced a stoichiometric amount of low molecular weight, highly isotactic poly(1-butene). ^{13}C NMR of the polymer shows saturated P−(*n*-butyl) and $CH_3CH(C_2H_5)$−P chain ends in approximately a 1:1 molar ratio. Peaks due to stereo- and regiodefects are below the level of detection, and olefinic protons are not observed in the ^1H NMR spectrum. The number-average degree of polymerization estimated by ^{13}C NMR is ca. 25, indicating activity of approximately 4% of the Hf centers.

(34) Landis, C. R.; Christianson, M. D. *Proc. Natl. Acad. Sci.* **2006**, *103*, 15349.
(35) Sillars, D. R. Ph.D. thesis, Univ. of Wisconsin, Madison, WI, 2003.
(36) Ducéré, J. M.; Cavallo, L. *Organometallics* **2006**, *25*, 1431, and references therein.
(37) For some examples of C_6F_5 transfer to metal, see: (a) Phomphrai, K.; Fenwick, A. E.; Sharma, S.; Fanwick, P. E.; Caruthers, J. M.; Delgass, W. N.; Abu-Omar, M. M.; Rothwell, J. P. *Organometallics* **2006**, *25*, 214. (b) Metcalfe, R. A.; Kreller, D. I.; Tian, J.; Kim, H.; Taylor, N. J.; Corrigan, J. F.; Collins, S. *Organometallics* **2002**, *21*, 1719. (c) Woodman, T. J.; Thornton-Pett, M.; Hughes, D. L.; Bochmann, M. *Organometallics* **2001**, *20*, 4080. (d) Guerin, F.; Stewart, J. C.; Beddie, C.; Stephan, D. W. *Organometallics* **2000**, *19*, 2994. (e) Scollard, J. D.; McConville, D. H.; Rettig, S. J. *Organometallics* **1997**, *16*, 1810. (f) Yang, X. M.; Stern, C. L.; Marks, T. J. *J. Am. Chem. Soc.* **1994**, *116*, 10015. For a recent theoretical work, see: Wondimagegn, T.; Xu, Z.; Vanka, K.; Ziegler, T. *Organometallics* **2004**, *23*, 3847, and references therein.

The number-average molecular weight (M_n) value of 950 g/mol, deduced from gel permeation chromatography (GPC), corresponds to approximately 6% active centers. The poly(1-butene) possesses a narrow polydispersity index of 1.2, consistent with "living" catalyst behavior and in line with the observed end groups. GC/MS analysis of the mother liquors after quenching shows ca. 10% of a fraction, consistent with a 1-butene-appended ligand (m/z = 568) and, more importantly, no evidence for 1-butene oligomers (C_8, C_{12}, C_{16}, etc.).

These results indicate that initiation is again much slower than propagation in this peculiar polymerization reaction. A simple kinetic scheme assuming that 5% of the catalysts are active and consume the remainder of the monomer leads to an estimate of the relative rate constants of 1000-fold for polymerization over activation. Since we have estimated that insertion into Hf−C_{Poly} is about an order of magnitude slower than insertion into the Hf−C_{Aryl},[39] these data suggest that the polymerization rates of catalysts of the **AI**-type are 4 orders of magnitude slower than those of the **BI**-type (for tetrakis-anions). Under the assumption that the *n*-butyl group is a reasonable model for the growing polymer chain,[36] the rate of the initial insertion into the Hf−C_{Butyl} bond is expected to be similar to the rate of polymerization. The simultaneous presence of a large fraction of uninitiated *n*-butyl cations **9a**/**b** and poly(1-butene) is not consistent with pathway A of Scheme 9. These data strongly suggest that *the active sites are **BI**-type species* from pathway B of Scheme 9, and that ***AI**-like ion pairs are not active or, at least, much less active for α-olefin polymerization*.

Conclusions

Our quest to develop a detailed mechanistic understanding of these pyridyl-amido complexes has uncovered a wealth of interesting activation chemistry centered on the unusual Hf−C_{Aryl} bond. Ascertaining the identity of the true active species remains of great interest considering the utility of these complexes in the production of specialty polyolefins. The data presented here provide direct NMR evidence concerning the preference for initial olefin insertion into the Hf−C_{Aryl} bond over the Hf−C_{Alkyl} bond. In the presence of a large excess of 1-hexene at low temperature, a **BI**-type monoinserted ion pair was directly observed and completely characterized. Computational studies including the FAB counterion showed that the kinetic product of insertion was the same as that observed experimentally. However, thermodynamically, this diastereomer is only the sixth most stable species out of eight possible α-olefin insertion products.

Calculations suggested chelating olefins, such as 2-vinylpyridine or 3-ethoxy-1-propylene, would insert into the Hf−C_{Aryl} bond in a 2,1-fashion to form a stable product. An analogous **BI** species was generated and fully characterized by the reaction of **2** with an equimolar amount of the chelating olefin, 2-vinylpyridine.[40] The simultaneous presence of Hf-Me and Hf-alkylaryl moieties in both of these examples confirms the relative ease of insertion into the Hf−C_{Aryl} bond. Insertion of 3-ethoxy-1-propylene led to complicated activation, but from computational studies and logic, one can deduce that insertion first goes through the Hf−C_{Aryl} bond.

Finally, the generation of precisely 1 equiv of 1-butene in close proximity to each metal center (i.e., perfect mixing) resulted in the formation of low molecular weight, highly isotactic poly(1-butene) rather than a stoichiometric insertion product or oligomers. These characteristics indicate the presence of a very low percentage of active metal centers, consistent with slow initiation relative to propagation. These data suggest that the active species is generated upon insertion of monomer into the Hf−C_{Aryl} bond.

Experimental Section

All manipulations were performed in flamed Schlenk-type glassware interfaced to a high-vacuum line ($< 10^{-5}$ Torr), or in a nitrogen-filled Vacuum Atmospheres glovebox ($<$ 1 ppm O_2). Molecular sieves (MS) were activated for 24 h at 200−230 °C under dynamic vacuum. All the solvents and liquid reagents were freeze−pump−thaw degassed on the high-vacuum line, dried over the appropriate drying agent, vacuum-transferred to a dry storage tube with a PTFE valve, and stored over activated MS. Benzene-d_6, toluene-d_8, pentane, hexane, toluene, and 3-ethoxy-1-propene were dried over Na/K alloy; 1,2-$F_2C_6H_4$ was refluxed for three days over P_2O_5 and finally dried over CaH_2; 2-vinylpyridine, chlorobenzene-d_5, and methylene chloride-d_2 were dried over CaH_2; 4-methyl-1-pentene and 1-hexene were dried over CaH_2 or $LiAlH_4$. $[HNMe_2Ph][B(C_6F_5)_4]$ and $[CPh_3][B(C_6F_5)_4]$ were obtained from Boulder Scientific Company and were used as received. $B(C_6F_5)_3$ was obtained from Boulder Scientific Company and was purified by sublimation (40−60 °C, 10^{-5} Torr). $HfCl_4$ (sublimed grade, 99.9+% Hf, $<$1.0% Zr) was purchased from Strem Chemical and used as received. *n*-BuLi (2.5 M solution in hexanes) and BuMgCl (2.0 M solution in diethyl ether) were purchased from Acros and Aldrich Chemical Co., respectively, and used as received.

NMR samples were prepared in oven-dried J-Young NMR tubes. ^{1}H, ^{13}C{^{1}H}, ^{1}H-COSY, ^{1}H-NOESY, ^{1}H-ROESY ^{1}H,^{13}C-HMQC, ^{1}H,^{13}C-HMBC, ^{19}F, and ^{19}F,^{1}H-HOESY NMR experiments were performed on a Bruker Avance DRX 400 instrument. Referencing by residual solvent signals is relative to TMS. Typical mixing time for the Overhauser experiments was in the range 120−800 ms. Complexes **1** and **2** were prepared as described previously.[10]

Generation of the Monoinserted Species 3. Complex **1** (7.2 mg, 0.01 mmol) and 1-hexene (0.21 mL, 1.7 mmol, 170 equiv) were dissolved in toluene-d_8 (see Figure 1S for the corresponding ^{1}H NMR spectrum at −56 °C) and cooled at −60 °C using an ethanol/liquid nitrogen bath. Then 0.20 mL of a toluene-d_8 solution containing $B(C_6F_5)_3$ (8 mg, 0.015 mmol) was injected into the NMR tube, and while shaking, the tube was quickly transferred to the NMR spectrometer (precooled to −56 °C). The polymerization was followed by ^{1}H NMR; 95% of 1-hexene was consumed after approximately 22 min, while resonances due to 1-hexene were not detectable after 40−50 min (see Figure 2S for ^{1}H NMR spectra taken approximately 2 min (black), 7 min (red), 15 min (blue), and 50 min (green) after the addition of $B(C_6F_5)_3$). When the olefin was completely consumed, the temperature inside the NMR probe was raised to −29 °C in order to obtain sharper resonances, and the organometallic complex present in solution was identified

(38) The relative fraction of 1-butene-appended ligand is estimated from uncorrected flame-ionization detection data.

(39) For the most likely pathway, the difference in these transition states was estimated at 2.2 kcal/mol with insertion into the Hf−C_{Aryl} bond lower than insertion into the Hf−C_{nButyl} bond (ref 9).

(40) Bijpost, E. A.; Zuideveld, M. A.; Meetsma, A.; Teuben, J. H. *J. Organomet. Chem.* **1998**, *551*, 159. For a more recent paper describing the use of 3-(methylthio)-1-propylene for similar studies see: Richter, B.; Meetsma, A.; Hessen, B.; Teuben, J. H. *Angew. Chem., Int. Ed.* **2002**, *41*, 2166.

as **3** by multinuclear and multidimensional NMR methods (Figures 4S−25S).

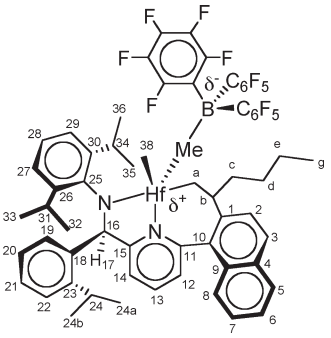

^{1}H NMR (C_7D_8, 244K, *J* values in Hz): δ 7.76 (d, $^3J_{HH}$ = 8.3, H3), 7.53 (d, $^3J_{HH}$ = 8.0, H5), 7.51 (d, $^3J_{HH}$ = 8.3, H2), 7.21 (m, H6 and H7), 7.14 (buried under solvent resonances, H8), 7.09 (buried under solvent resonances, H19), 6.95 (m, H28 and H29), 6.86 (m, H20, H21, and H22), 6.60 (t, $^3J_{HH}$ = 7.8, H13), 6.51 (d, $^3J_{HH}$ = 7.8, H14), 6.42 (m, H12 and H27), 6.16 (s, H17), 3.83 (brm, Hb), 3.22 (sept, $^3J_{HH}$ = 6.7, H34), 2.89 (sept, $^3J_{HH}$ = 6.7, H31), 2.71 (sept, $^3J_{HH}$ = 6.7, H24), 2.48 (br, Me-B), 1.38 (buried under polymer resonances, Ha and Ha′), 1.25 (buried under polymer resonances, H36), 1.15 (buried under polymer resonances, H35), 1.08 (buried under polymer resonances, H24a), 0.97 (buried under polymer resonances, Hd), 0.79 (buried under polymer resonances, Hd′), 0.78 (buried under polymer resonances, Hc), 0.77 (d, $^3J_{HH}$ = 6.7, H32), 0.75 (m, Hg), 0.58 (m, Hc′), 0.31 (d, $^3J_{HH}$ = 6.7, H24b), 0.06 (s, H38), −0.28 (d, $^3J_{HH}$ = 6.7, H33). ^{13}C{^{1}H} NMR (C_7D_8, 244 K): δ 167.5 (s, C15), 155.1 (s, C11), 147.1 (s, C23), 146.4 (s, C26), 145.7 (s, C30), 143.3 (s, C1), 140.6 (s, C13), 139.3 (s, C25), 138.4 (s, C18), 133.6 (s, C9), 133.3 (s, C10), 132.6 (s, C3), 129.9 (s, C2), 129.6 (s, C5), 129.3 (s, C19), 129.1 (s, C20, C21 or C22), 128.4 (s, C28), 127.5 (s, C12), 127.5 (s, C20, C21 or C22), 127.3 (s, C4), 126.3 (s, C6 and C7), 126.2 (s, C20, C21 or C22), 125.4 (s, C29), 125.3 (s, C27), 123.9 (s, C8), 123.1 (s, C14), 78.1 (s, Ca), 72.4 (s, C16), 60.6 (s, C38), 48.0 (s, Cb), 39.6 (s, Me-B), 36.6 (s, *Cc*), 30.6 (s, Cd), 28.8 (s, C24), 28.6 (s, C34), 28.5 (s, C31), 26.1 (s, C35), 25.4 (s, C36), 24.7 (s, C33), 24.5 (s, C24a), 24.0 (s, C32), 23.4 (s, Ce), 23.1 (s, C24b), 14.3 (s, Cg). ^{19}F NMR (C_7D_8, 244 K *J* values in Hz): δ −133.44 (brd, $^3J_{FF}$ = 23.2, *o*-F), −159.87 (t, $^3J_{FF}$ = 21.3, *p*-F), −164.51 (m, *m*-F).

Generation of Complex 4. Complex **2** (30 mg, 0.0244 mmol) was dissolved in C_6D_6 (0.7 mL), and 3-ethoxy-1-propene (8 μL, 0.0730 mmol) was added in one portion. After 3 h a deep-yellow-orange oil separated from the solution. The supernatant was removed and the oil redissolved in C_6D_6/C_6D_5Cl for NMR analysis.

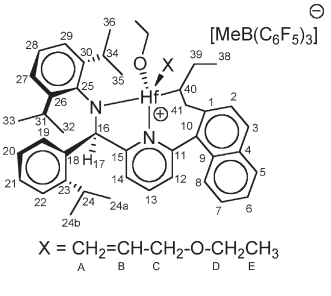

^{1}H NMR (C_6D_6/C_6D_5Cl, 298 K, *J* values in Hz): δ 7.73 (d, $^3J_{HH}$ = 8.0, H5), 7.70 (d, $^3J_{HH}$ = 8.5, H3), 7.54 (d, $^3J_{HH}$ = 8.4, H8), 7.40 (m, H6), 7.33 (m, H7), 7.21 (d, $^3J_{HH}$ = 7.7, H13), 7.19 (d, $^3J_{HH}$ = 8.5, H2), 7.08 (m, H29), 7.06−6.90 (m, H20, H21, H22, and H28), 6.81 (m, H12 and H27), 6.72 (d, $^3J_{HH}$ = 7.7, H14), 6.41 (s, H17), 6.37 (m, H19), 4.95 (m, H_A), 4.79 (m, HA and H_B), 3.39 (m, H34, H41, and H_C), 3.23 (m, HC), 3.17 (m, HfO***CH*****$_2$**CH_3), 3.08 (m, H_D), 2.97 (m, HfO***CH*****$_2$**CH_3), 2.87 (m, H_D), 2.66 (sept, $^3J_{HH}$ = 6.7, H24), 2.46 (sept, $^3J_{HH}$ = 6.7, H31), 2.28 (dd, $^2J_{HH}$ = 13.7, $^3J_{HH}$ = 6.8, H41), 2.10 (m, H39), 1.68 (m, H39), 1.45 (m, H40),1.41 (d, $^3J_{HH}$ = 6.7, H36), 1.28 (d, $^3J_{HH}$ = 6.7, H35), 1.19 (br, Me-B), 1.13 (t, $^3J_{HH}$ = 7.1, H38), 1.10 (d, $^3J_{HH}$ = 6.7, H24a), 0.77 (d, $^3J_{HH}$ = 6.7, H32), 0.61 (t, $^3J_{HH}$ = 7.1, H_E), 0.48 (t, $^3J_{HH}$ = 7.1, HfOCH$_2$***CH*****$_3$**), 0.44 (d, $^3J_{HH}$ = 6.7, H24b), 0.13 (d, $^3J_{HH}$ = 6.7, H33). ^{13}C{^{1}H} NMR (C_6D_6/C_6D_5Cl, 298 K): δ 169.9 (s, C15), 155.8 (s, C11), 149.6 (s, C23), 145.27 (s, C26), 145.23 (s, C26), 144.8 (s, C30), 142.7 (s, C1), 141.4 (s, C13), 139.2 (s, C18), 133.7 (s, C4), 132.0 (s, C3), 131.9 (s, C9), 130.7 (s, C10), 130.67 (s, C19), 130.0 (s, C2), 129.8 (s, C5), 129.1 (s, C7), 128.0 (s, C6), 127.8 (s, C_A), 127.0 (s, C12 and C28), 127.4, 127.1, 127.0 (s, C20, C21, C22, C_B), 125.6 (s, C29), 125.4.3 (s, C14), 125.2 (s, C27), 124.9 (s, C8), 77.6 (s, C40), 76.6 (s, C_C), 72.5 (s, C_D), 72.1 (s, C16), 67.7 (s, HfO***CH*****$_2$**CH_3), 36.3 (s, C41), 29.5 (s, C31), 29.3 (s, C24), 29.07 (s, C34), 27.9 (s, C35), 27.1 (s, C39), 26.3 (s, C24a), 26.27 (s, C32), 25.0 (s, C36), 23.7 (s, C33), 22.3 (s, C24b), 18.1 (s, HfOCH$_2$***CH*****$_3$**), 16.3 (s, C38), 13.7 (s, C_E). ^{19}F NMR (C_6D_6/C_6D_5Cl, 298 K, *J* values in Hz): δ −132.16 (brd, $^3J_{FF}$ = 20.7, *o*-F), −164.7 (t, $^3J_{FF}$ = 21.0, *p*-F), −167.2 (m, *m*-F).

Synthesis of Complex 6. Complex **2** (15 mg, 0.0122 mmol) was charged into a J-Young NMR tube and dissolved using a mixture of C_7D_8 and C_6D_5Cl (0.7 mL). 2-Vinylpyridine (66 μL, of a 0.184 M solution in toluene-d_8, 0.0122 mmol) was added in three portions. The mixture was allowed to react for a few minutes, and then all the volatiles were removed under vacuum. The residue was then redissolved in C_6D_5Cl and analyzed by NMR. Complex **6** can be isolated as a deep orange oil starting from 70 mg of **2** and performing the reaction in neat C_7D_8. Several attempts to grow single crystals of **6** suitable for X-ray analysis were unsuccessful thus far (^{1}H and ^{13}C NMR spectra of **6** are reported in the Supporting Information, Figures 29S−38S).

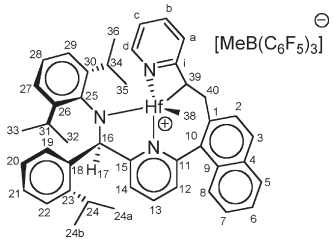

^{1}H NMR (C_6D_5Cl, 298 K, *J* values in Hz): δ 7.71 (d, $^3J_{HH}$ = 8.3, H3), 7.65 (d, $^3J_{HH}$ = 8.1, H5), 7.63 (d, $^3J_{HH}$ = 8.0, Ha), 7.58 (d, $^3J_{HH}$ = 7.9, H13), 7.46 (dt, $^3J_{HH}$ = 8.0, $^4J_{HH}$ = 1.7, Hb), 7.38 (m, H7), 7.33 (m, H6), 7.28 (d, $^3J_{HH}$ = 8.3, H2), 7.18 (m, Hd), 7.17−7.10 (m, H12, H14, H20, H22, H28, and H29), 7.03 (d, $^3J_{HH}$ = 8.2, H8), 7.02−6.96 (m, H19, H21, H27), 6.57 (s, H17), 6.38 (m Hc), 4.06 (d, $^2J_{HH}$ = 14.8, H40eq), 3.31 (dd, $^2J_{HH}$ = 14.8, $^3J_{HH}$ = 8.1, H40ax), 3.18 (sept, $^3J_{HH}$ = 6.7, H31), 3.09 (sept, $^3J_{HH}$ = 6.7, H34), 2.89 (sept, $^3J_{HH}$ = 6.7, H24), 2.13 (d, $^3J_{HH}$ = 8.1, H39), 1.42 (d, $^3J_{HH}$ = 6.7, H36), 1.24 (d, $^3J_{HH}$ = 6.7, H24a), 1.17 (br, Me-B), 0.90 (d, $^3J_{HH}$ = 6.7, H32), 0.74 (d, $^3J_{HH}$ = 6.7, H35), 0.54 (d, $^3J_{HH}$ = 6.7, H24b), 0.13 (d, $^3J_{HH}$ = 6.7, H33), −1.01 (s, H38). ^{13}C{^{1}H} NMR (C_6D_5Cl, 298 K): δ 167.8 (s, C15), 163.3 (s, Ci), 154.1 (s, C11), 149.3 (s, C26), 148.7 (s, C30), 147.7 (s, C23), 145.1 (s, Cd), 143.1 (s, Cb), 142.7 (s, C13), 138.9 (s, C1), 137.2 (s, C18), 134.0 (s, C9), 133.1 (s, C4), 132.2 (s, C3), 131.3 (s, C25), 129.1 (s, C5), 129.0 (s, C19), 128.6 (s, C7), 127.2 (s, C2), 126.7 (s, C6), 124.9 (s, Ca), 123.2 (s, C8), 119.3 (s, *Cc*), 129.57, 129.54, 128.56, 127.29, 126.77, 126.12, 124.97, 124.51 (s, C12, C14, C20, C21, C22, C27, C28, C29), 70.4 (s, C16), 64.8 (s, C39), 61.3 (s, C38), 31.6 (s, C40), 28.69 (s, C24), 28.66 (s, C32), 28.63 (s, C34), 28.2 (s, C31), 24.9 (s, C24a), 24.7

(s, C35), 24.5 (s, C36), 23.1 (s, C33), 22.7 (s, C24b), 11.0 (v br, Me-B). ^{19}F NMR (C_6D_5Cl, 298 K, *J* values in Hz): δ −132.09 (brd, $^3J_{FF}$ = 20.7, *o*-F), −164.8 (t, $^3J_{FF}$ = 21.0, *p*-F), −167.2 (m, *m*-F).

Generation of Ion Pair 7. Inside the glovebox, an NMR tube containing a solution of **6** in C_6D_5Cl was treated with a solution of 2-vinylpyridine in C_6D_5Cl (1 equiv). NMR analysis showed complete consumption of **6** and formation of complex **7**. Alternatively, complex **7** may be conveniently obtained by adding 2 equiv of 2-vinylpyridine to a solution of ion pair **2**.

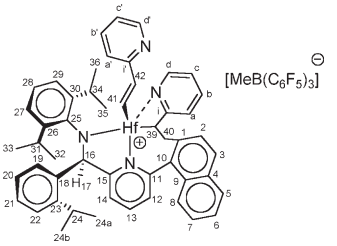

^{1}H NMR (C_6D_6/C_6D_5Cl, 298 K, *J* values in Hz): δ 7.72−7.65 (m, H8 and H5), 7.63 (d, $^3J_{HH}$ = 8.2, H3), 7.54 (brd, $^3J_{HH}$ = 8.2, Ha), 7.45−735 (m, Hb, H6, and H7), 7.32 (t, $^3J_{HH}$ = 7.9, H13), 7.25 (m, H21), 7.19 (d, $^3J_{HH}$ = 8.2, H2), 7.19−7.15 (m, H20, H22, and H28), 7.12 (m, H19), 7.09 (d, $^3J_{HH}$ = 14.5, H41), 7.00−7.03 (m, H12, H14, and Hb′), 7.00 (dd, $^3J_{HH}$ = 7.9, $^4J_{HH}$ = 1.7, H27), 6.93 (dd, $^3J_{HH}$ = 7.7, $^4J_{HH}$ = 1.6, H29), 6.74 (s, H17), 6.68 (m, Hd), 6.64 (m, Hd), 6.60 (d, $^3J_{HH}$ = 14.5, H42), 6.46 (m, Hc), 6.39 (m, Hc′), 6.32 (brd, $^3J_{HH}$ = 7.9, Ha′), 4.39 (d, $^2J_{HH}$ = 13.9, H40), 3.55 (dd, $^2J_{HH}$ = 13.9, $^3J_{HH}$ = 5.9, H40), 3.23 (sept, $^3J_{HH}$ = 6.7, H34), 3.91 (sept, $^3J_{HH}$ = 6.7, H31), 2.78 (sept, $^3J_{HH}$ = 6.7, H24), 2.15 (d, $^3J_{HH}$ = 5.9, H39), 1.35 (d, $^3J_{HH}$ = 6.7, H36), 1.32 (br, Me-B), 1.25 (d, $^3J_{HH}$ = 6.7, H24a), 0.81 (d, $^3J_{HH}$ = 6.7, H32), 0.59 (d, $^3J_{HH}$ = 6.7, H24b), 0.16 (d, $^3J_{HH}$ = 6.7, H33), 0.02 (d, $^3J_{HH}$ = 6.7, H35). ^{13}C{^{1}H} NMR (C_6D_6/C_6D_5Cl, 298 K): δ 212.7 (s, C41), 171.1 (s, Ci), 168.5 (s, C15), 160.6 (s, Ci′), 155.7 (s, C11), 148.9 (s, C23), 147.9 (s, Cd′), 147.1 (s, C26), 146.8 (s, C30), 145.1 (s, Cd), 145.0 (s, C42), 142.5 (s, Cb), 142.4 (s, Cb′), 142.2 (s, C25), 140.18 (s, C18), 140.17 (s, C13), 139.2 (s, C1), 133.9 (s, C4), 133.6 (s, C9), 132.2 (s, C10), 131.5 (s, C3), 130.4 (s, C19), 129.9 (s, C5), 129.6 (s, C2), 129.0 (s, C6 or C7), 128.9 (s, C12), 128.5 (s, C28), 127.7 (s, C20 or C21), 127.4 (s, C29), 127.2 (s, C22 and C7 or C6), 126.1 (s, Ca), 125.9 (s, C8), 125.3 (s, C27), 124.9 (s, C14), 124.1 (s, Ca′), 122.9 (s, Cc′), 121.1 (s, Cc), 72.9 (s, C16), 61.0 (s, C39), 35.9 (s, C40), 29.4 (s, C31), 29.3 (s, C24), 28.3 (s, C34), 26.8 (s, C32), 26.5 (s, C36), 26.3 (s, C24a), 24.12 (s, C33), 24.09 (s, C35), 22.6 (s, C24b), 11.5 (v br, Me-B). ^{19}F NMR (C_6D_6/C_6D_5Cl, 298 K, *J* values in Hz): δ −132.1 (brd, $^3J_{FF}$ = 20.7, *o*-F), −164.6 (t, $^3J_{FF}$ = 21.0, *p*-F), −167.05 (m, *m*-F).

Synthesis of Complex 8. A glass jar was charged with 5.2 mmol of ligand dissolved in 30 mL of toluene. To this solution was added 5.40 mmol of *n*-BuLi (2.5 M solution in hexanes, Acros) by syringe. This solution was stirred for 30 min, and the toluene was removed using a vacuum system attached to the drybox. Hexane was added, removed by vacuum, and added again, and the resulting slurry was filtered to give a tan solid. A glass jar was then charged with the tan solid dissolved in 30 mL of toluene. To this solution was added 5.0 mmol of solid $HfCl_4$. The jar was capped with an air-cooled reflux condenser, and the mixture was heated at reflux for about 4 h. After cooling, 18.1 mmol of BuMgCl (3.5 equiv, 2.0 M solution in diethyl ether, Aldrich Chemical Co.) was added by syringe, and the resulting mixture was stirred overnight at ambient temperature. Solvent (toluene and diethyl ether) was removed from the reaction mixture by vacuum. Hexane (30 mL) was added to the residue, the mixture was filtered, and the residue (magnesium salts) was washed with additional hexane (30 mL). Solvent was removed by vacuum from the combined hexane solutions to give the desired product as a yellow solid: 3.2 g; 80%.

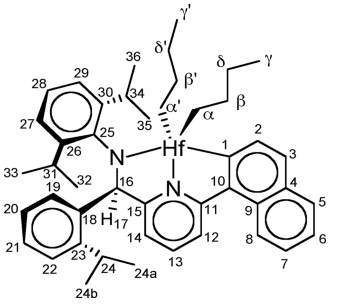

^{1}H NMR (C_7D_8, 298 K, *J* values in Hz): δ 8.71 (d, $^3J_{HH}$ = 7.6, H2), 8.19 (m, H8), 7.77 (d, $^3J_{HH}$ = 7.6, H3), 7.67 (m, H5), 7.48 (d, $^3J_{HH}$ = 8.0, H12), 7.39 (m, H19), 7.26 (m, H7 and H6), 7.15 (dd, $^3J_{HH}$ = 7.5, $^4J_{HH}$ = 1.9, H29), 7.1−7.0 (m, H20, H21, H22, H27, and H28), 6.88 (d, $^3J_{HH}$ = 8.0, H13), 6.61 (d, $^3J_{HH}$ = 8.0, H14), 6.58 (s, H17), 3.75 (sept, $^3J_{HH}$ = 6.7, H31), 3.36 (sept, $^3J_{HH}$ = 6.7, H34), 2.91 (sept, $^3J_{HH}$ = 6.7, H24), 2.09 (m, H_β), 1.85 (m, $H_{\beta'}$), 1.49 (m, H_α), 1.41 (m, H36 and H32), 1.55 (m, H_γ and $H_{\gamma'}$), 1.26 (m, H_α), 1.20 (d, $^3J_{HH}$ = 6.7, H24a), 1.18 (d, $^3J_{HH}$ = 6.7, H35), 1.07 (m, $H_{\alpha'}$), 0.86 (t, $^3J_{HH}$ = 7.3, H_δ or $H_{\delta'}$), 0.84 (t, $^3J_{HH}$ = 7.3, $H_{\delta'}$ or H_δ), 0.82 (m, $H_{\alpha'}$), 0.67 (d, $^3J_{HH}$ = 6.7, H24b), 0.31 (d, ^3JHH = 6.7, H33). ^{13}C{^{1}H} NMR (C_7D_8, 298 K): δ 205.5 (s, C1), 170.7 (s, C15), 164.4 (s, C11), 147.5 (s, C26), 146.8 (s, C23), 146.4 (s, C30), 146.3 (s, C25), 144.2 (s, C10) 141.5 (s, C18), 140.6 (s, C13), 135.6 (s, C4), 134.6 (s, C2), 130.8 (s, C9), 130.4 (s, C19), 129.8 (s, C5), 129.7 (s, C3), 129.3, 128.8, 128.0, 126.8, 125.9 (s, C20, C21, C22, C27 and C28), 126.7 (s, C7), 125.3 (s, C6), 124.9 (s, C29), 124.1 (s, C8), 120.5 (s, C12), 119.4 (s, C14), 88.3 (s, Cα'), 83.6 (s, Cα), 76.9 (s, C16), 30.6 (s, Cβ'), 30.22 (s, Cβ), 30.18 (s, Cγ or Cγ'), 29.6 (s, Cγ' or Cγ), 28.7 (s, C24), 28.6 (s, C34), 28.3 (s, C31), 27.0 (s, C32), 26.2 (s, C36), 25.5 (s, C35), 25.2 (s, C24a), 24.2 (s, C33), 23.1 (s, C24b), 14.2 (s, Cδ), 14.1 (s, Cδ').

Isolation of Poly-1-butene from Scale-up Activation of 8 with $[CPh_3][B(C_6F_5)_4]$. A 36 mL portion of a 0.0846 mM solution of **6** in methylcyclohexane (2.445 g, 3.05 mmol) was charged in a 250 mL flask equipped with a PTFE valve inside the glovebox. The flask was connected to the high-vacuum line and the solvent removed under reduced pressure. Inside the glovebox, 2.80 g of $[CPh_3][B(C_6F_5)_4]$ was added in the flask and approximately 80 mL of dry toluene was added in one portion under magnetic stirring. After 45 min the flask was taken out from the glovebox and connected to the high-vacuum line, where the solvent was removed under reduced pressure. The foamy residue was scratched with a spatula while the flask was open to the air. Regular toluene (ca. 25 mL) was added in one portion, and the mixture was vigorously stirred for few minutes. After a while, a dark red-brown oily phase separated from the solution. The oil (fraction 1) was separated from the solution by means of a Pasteur pipet. The solution was concentrated to approximately 10−15 mL, resulting in the separation of an additional amount of oil. The last oily phase (fraction 2) was separated from the residual solution (fraction 3) by centrifugation. Fraction 3 was poured in a flask and the solvent removed under vacuum. Workup of fraction 2: approximately 200 mL of acidified MeOH was added to the oil. The resulting cloudy suspension was filtered. The mother liquor (fraction 2A) was stored in open air to allow solvent evaporation. The solid residue on the frit was redissolved in CH_2Cl_2 and transferred to a small vial, where the solvent was removed by N_2 flush. Approximately 3 mL of MeOH was added to the solid residue; the suspension was vigorously shaken by sonication and then stored at −20 °C overnight. Finally, the solid (fraction 2B) was collected by

centrifugation, washed with 1 mL of MeOH, and dried overnight under vacuum (12 mg was obtained). Workup of fraction 3: approximately 150 mL of MeOH (to which 3 drops of 37% aqueous HCl was added) was poured in the flask containing the solid residue. The resulting suspension was filtered. The mother liquor (fraction 3A) was stored in open air to allow solvent evaporation. The solid residue on the frit was redissolved in CH_2Cl_2 and transferred to a small vial, where the solvent was removed by N_2 flush. Approximately 3 mL of MeOH was added to the solid residue; the suspension was vigorously shaken by sonication and then stored at −20 °C overnight. Finally, the solid (fraction 3B) was collected by centrifugation, washed with 1 mL of MeOH, and dried overnight under vacuum (60 mg was obtained). According to subsequent characterization, fractions 2B and 3B turned out to poly-1-butene samples with identical characteristics. The theoretical yield in polymers (or oligomers) ranges from 171 (virtually 0% active sites) to 342 mg (virtually 100% active sites). ^{13}C NMR spectrum and GPC data are reported in the Supporting Information, Figures 39S and 40S, respectively.

Acknowledgment. We thank Roger Kuhlman, Timothy Wenzel, James Stevens, Daryoosh Beigzadeh, and Harold Boone for helpful discussions and the Ministero dell'Università e della Ricerca (MUR, Rome, Italy; PRIN 2007) and The Dow Chemical Company for support.

Supporting Information Available: Additional NMR data and computational details. This material is available free of charge via the Internet at http://pubs.acs.org.